

ORIGINAL ARTICLE

Cytotoxic effects of Mn(III) N-alkylpyridylporphyrins in the presence of cellular reductant, ascorbate

XIAODONG YE^{1*}, DIANE FELS², ARTAK TOVMASYAN², KATHERINE M. AIRD^{3,4}, CASEY DEDEUGD², JENNIFER L. ALLENSWORTH^{3,4}, IVAN KOS^{2#}, WON PARK², IVAN SPASOJEVIC⁵, GAYATHRI R. DEVI^{3,4}, MARK W. DEWHIRST², KAM W. LEONG¹ & INES BATINIC-HABERLE²

¹Department of Biomedical Engineering, Duke University, Durham, NC, USA, ²Department of Radiation Oncology, Duke University Medical Center, Durham, NC, USA, ³Department of Surgery, Duke University Medical Center, Durham, NC, USA, ⁴Department of Pathology Duke University Medical Center, Durham, NC, USA, and ⁵Department of Medicine, Duke University Medical Center, Durham, NC, USA

(Received date: 27 May 2011; Accepted date: 14 August 2011)

Abstract

Due to the ability to easily accept and donate electrons Mn(III)N-alkylpyridylporphyrins (MnPs) can dismutate O₂^{•-}, reduce peroxynitrite, but also generate reactive species and behave as pro-oxidants if conditions favour such action. Herein two *ortho* isomers, MnTE-2-PyP⁵⁺, MnTnHex-2-PyP⁵⁺, and a *meta* isomer MnTnHex-3-PyP⁵⁺, which differ greatly with regard to their metal-centered reduction potential, E_{1/2} (Mn^{III}P/Mn^{II}P) and lipophilicity, were explored. Employing Mn^{III}P/Mn^{II}P redox system for coupling with ascorbate, these MnPs catalyze ascorbate oxidation and thus peroxide production. Consequently, cancer oxidative burden may be enhanced, which in turn would suppress its growth. Cytotoxic effects on Caco-2, Hela, 4T1, HCT116 and SUM149 were studied. When combined with ascorbate, MnPs killed cancer cells *via* peroxide produced outside of the cell. MnTE-2-PyP⁵⁺ was the most efficacious catalyst for peroxide production, while MnTnHex-3-PyP⁵⁺ is most prone to oxidative degradation with H₂, and thus the least efficacious. A 4T1 breast cancer mouse study of limited scope and success was conducted. The tumour oxidative stress was enhanced and its microvessel density reduced when mice were treated either with ascorbate or MnP/ascorbate; the trend towards tumour growth suppression was detected.

Keywords: Mn porphyrin, cancer cells, ascorbate, SOD mimics, oxidative stress, MnTE-2-PyP⁵⁺

Abbreviations: Charges in the MnP abbreviations are omitted throughout descriptions of Figures; MnPs, Mn(III) N-alkylpyridylporphyrins; SOD, superoxide dismutase; ROS, reactive oxygen species; RNS, reactive nitrogen species; RS, reactive species; ONOO⁻, peroxynitrite; O₂^{•-}, superoxide; •OH, hydroxyl radical; Asc was used as a general term with no intention to account for its protonation or redox equilibria; H₂A, fully protonated ascorbic acid; A, dehydroascorbic acid; HA⁻, monodeprotonated ascorbate; HA•, ascorbyl radical; A⁻, deprotonated ascorbyl radical; Mn^{III}P⁵⁺ and Mn^{II}P⁴⁺, oxidized (Mn + 3 oxidation state) and reduced Mn porphyrin (Mn + 2 oxidation state), total charge 5+ and 4+ are omitted in text; MnTM-4-PyP⁵⁺, Mn(III) meso-tetrakis(N-methylpyridinium-4-yl)porphyrin; MnTE-2-PyP⁵⁺, AEOL10113, FBC-007, Mn(III) meso-tetrakis(N-ethylpyridinium-2-yl)porphyrin; MnTE-3-PyP⁵⁺, Mn(III) meso-tetrakis(N-ethylpyridinium-3-yl)porphyrin; MnTnHex-2-PyP⁵⁺, Mn(III) meso-tetrakis(N-n-hexylpyridinium-2-yl)porphyrin; MnTnHex-3-PyP⁵⁺, Mn(III) meso-tetrakis(N-n-hexylpyridinium-3-yl)porphyrin; DMF, N,N-dimethylformamide; DMSO, dimethyl sulfoxide; TMRE, tetramethylrhodamine ethyl ester, perchlorate; R_f, thin-layer chromatographic retention factor that presents the ratio

Present address/affiliation: #Ivan Kos, Faculty of Pharmacy and Biochemistry, University of Zagreb, A. Kovacica 1, 10 000 Zagreb, Croatia. *Xiaodong Ye, Department of Chemical Physics, University of Science and Technology of China, 96 Jinzhai Road, Hefei, Anhui 230026, P. R. China.

Correspondence: Ines Batinic-Haberle, Department of Radiation Oncology, Duke University Medical Center, Research Drive, 281b/285 MSRB I, Box 3455, Durham, NC 27710. Tel: 919-684-2101. Fax: 919-684-8718. E-mail: ibatinic@duke.edu

between the solvent and compound path in 1:1:8=KNO_{3(sat)}:H₂O:CH₃CN solvent system; P_{OW} , partition between *n*-octanol and water; $E_{1/2}$, half-wave reduction potential for Mn^{III}P/Mn^{II}P redox couple; SOD, superoxide dismutase; NHE, normal hydrogen electrode; HIF-1 α , hypoxia inducible factor-1, NF- κ B, nuclear factor κ B; AP-1, activator protein-1; SP-1, specificity protein 1; TNF- α , tumour necrosis factor- α ; VEGF, vascular endothelial growth factor; EGF, epidermal growth factor; MCP-1, monocyte chemotactic protein-1; HER2, human epidermal growth factor receptor 2; IBC, inflammatory breast cancer; fL, femtoLiter; PBS, phosphate buffered saline; ip, intraperitoneal; sc, subcutaneous; DMEM, Dulbecco's Modified Eagle Medium; EBS, fetal bovine serum.

Introduction

Those Mn(III) *N*-alkylpyridylporphyrins (MnPs) (Figure 1) which have metal-centered reduction potential, $E_{1/2}$ for Mn^{III}P/Mn^{II}P redox couple around +300 mV, alike SOD enzymes, are equally able to efficiently reduce and oxidize superoxide, O₂^{•-}. Thus, MnPs: (a) are powerful catalysts of O₂^{•-} dismutation, and mimic SOD enzymes which are the first-line of endogenous antioxidative defenses [1–5]; and (b) bear potential to be pro-oxidants. The ability of MnP to dismutate O₂^{•-} parallels its ability to reduce ONOO⁻, and to modulate cellular transcriptional activity [1–5]. MnPs can *in vivo* adopt 4 oxidation states, +2, +3, +4 and +5. The pro-oxidative action can arise directly or indirectly from all four oxidation states. During the facile reduction from Mn^{III}P to Mn^{II}P, they could oxidize cellular redox-able low-molecular weight compounds and proteins as well as O₂^{•-}. In a reduced state, Mn^{II}P could reduce O₂^{•-}, or bind oxygen and reduce it to O₂^{•-}. Subsequently, H₂O₂ will be formed which could act as oxidant in its own right, but could also affect signalling pathways, perpetuating oxidative stress [6–8]. Under physiological conditions peroxide will be removed by abundant peroxide-removing enzymes such as catalases, glutathione peroxidases, glutathione reductases, glutathione transferases, thioredoxins, peroxyredoxins, etc. The O=Mn^{IV}P and O=Mn^VP are strong oxidants in their own right also, and were reportedly formed in the reaction of Mn^{III}P and Mn^{II}P with ONOO⁻ [9–11].

We have already shown in an *E. coli* model that MnPs become pro-oxidants in the presence of cellular

reductant ascorbate [12]. In that model MnPs alone are able to substitute for the lack of cytosolic SODs and allow SOD-deficient *E. coli* to grow aerobically as well or better than the wild type [1,3]. However, in the presence of ascorbate, MnPs catalyzed ascorbate-driven H₂O₂ formation. The increased peroxide levels forced *E. coli* to fight back/adapt *via* induction of *oxyR* regulon, and upregulation of peroxidases and catalases [12,13].

Our earlier understanding was that the inhibition of transcription factor activation is due to the removal of signalling reactive species by MnPs [1–5]. However, Tse et al [14] and Jaramillo et al [15,16] have shown that the ability of MnPs to prevent activation of the master transcription factor, NF- κ B, could be pro-oxidative in nature also [14–16]. The oxidation of p50 subunit of NF- κ B in the nucleus [14,17,18] and/or glutathionylation of p65 subunit in the cytosol in the presence of glutathione and H₂O₂ has been suggested to result from the pro-oxidative action of MnP (Figure 2). In the latter case, MnTE-2-PyP⁵⁺ enhances anticancer effects of glucocorticoids in a lymphoma study [15,16]. Growing number of studies have recognized the glutathionylation as a major modification of critical proteins [16,19–24]. In our earlier mouse studies on the inhibitory effect of MnTE-2-PyP⁵⁺ on transcription factors HIF-1 α and AP-1, the removal of signalling reactive species was offered as an explanation [25,26]. It may well be that the protein cysteine modification, observed with NF- κ B subunits, is operative with HIF-1 α and AP-1 also. Importantly, the data on transcription factors warn us to distinguish between the mecha-

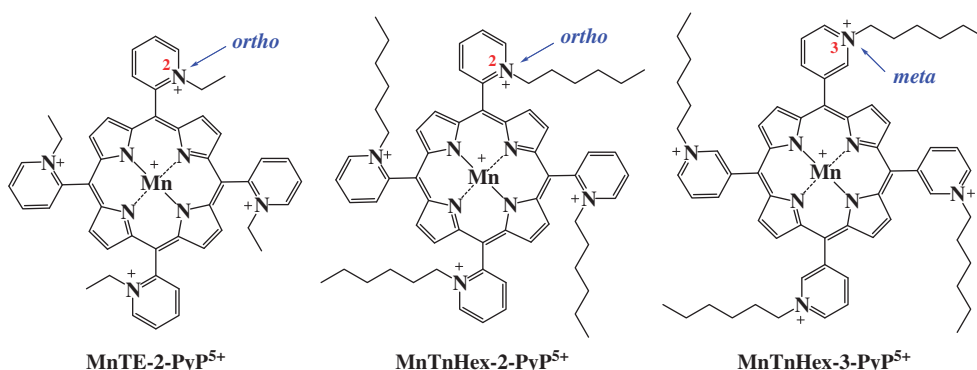


Figure 1. Structures of three manganese porphyrins (MnPs) studied: MnTE-2-PyP⁵⁺, MnTnHex-2-PyP⁵⁺ and MnTnHex-3-PyP⁵⁺. Ortho(2) and meta(3) positions of nitrogen atoms in pyridyl rings are indicated.

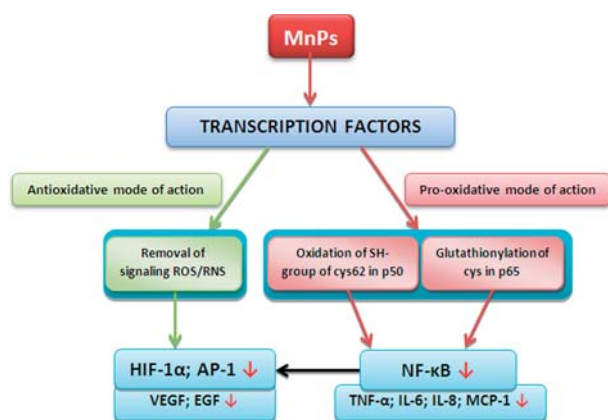


Figure 2. The mechanism of action of MnPs upon transcription factors was reported to be anti- and pro-oxidative. In a cellular study it was shown that treatment of 4T1 cells with H_2O_2 or $\cdot NO$ donor activates HIF-1 α while the activation was fully inhibited in the presence of MnTE-2-PyP $^{5+}$ [25]. With AP-1 again, the inhibition of its activation was ascribed to the removal of ROS/RNS [26]. With NF- κ B convincing evidence was provided to conclude that the NF- κ B subunits, p50 (in the nucleus) [4,14,17,18,27] and/or p65 (in the cytosol, in the presence of GSH and H_2O_2), were oxidatively damaged by MnTE-2-PyP $^{5+}$; glutathionylation was suggested in the latter case [15,16,19,27]. Glutathionylation has been increasingly reported as a critical protein cysteine modification [16,19–24]. The same modification could have happened with HIF-1 α and AP-1. HIF-1 α is reportedly under the control of NF- κ B also [28].

nism of MnP action and the effects observed. For example, in a diabetes model, MnP presumably acted *via* pro-oxidative mechanism, while the beneficial effects observed were clearly of antioxidative nature [27]. The type of MnP action, anti- or pro-oxidative (Figure 2), would depend upon the cellular levels of reactive species and antioxidants, cellular ratio of superoxide- to peroxide-removing systems, levels of oxygen, and cellular and subcellular distribution of MnP. It would also depend whether the normal cell (with abundant peroxide-removing enzymes) or the cancer cell (with compromised oxidative status and different transcription factor profile) is considered.

The metalloporphyrins (exogenous and endogenous) or other redox-cycling agents were shown with a few other laboratories also, to catalyze the ascorbate-driven H_2O_2 production *in vivo* and *in vitro*, and in turn exert anticancer effects [6,29–34]. Such studies are highly relevant due to the high endogenous intracellular levels of ascorbate. Several groups are already exploring the clinical anticancer potential of ascorbate in the presence and absence of redox-cycling agent [35–38]. The use of ascorbate/menadione system is already in clinic [35,39].

Mn(III) *N*-alkylpyridylporphyrins differ vastly with respect to the metal-centered reduction potential for the Mn^{III}P/Mn^{II}P redox couple, $E_{1/2}$, and lipophilicity (Table I). The $E_{1/2}$ shows which oxidation state of a porphyrin Mn site (+3 in Mn^{III}P $^{5+}$ or +2 in Mn^{II}P $^{4+}$) is a stable one, *i.e.* $E_{1/2}$ shows the affinity of Mn^{III}P towards reduction to Mn^{II}P. Structure–activity relationship studies showed that $E_{1/2}$ is linearly related to $\log k_{cat}(O_2^{\cdot-})$ and is thus also an indicator of SOD-like potency of MnP [1–5]. Finally, $E_{1/2}$ determines the MnP stability towards oxidative degradation with H_2O_2 , whose ascorbate-driven production it catalyzes. The $E_{1/2}$ of *meta* isomers is up to 300 mV more negative than the $E_{1/2}$ of *ortho* isomers. Thus *meta* isomers, which favour Mn +3 oxidation state, are not as easily reduced as *ortho* analogs; upon reduction they readily reoxidize whereby producing H_2O_2 which in turn degrades them (Table I) [1,2,40–43]. Upon reduction of Mn^{III}P to Mn^{II}P, the single charge from the metal site gets lost, which vastly enhances the MnP lipophilicity. The gain in lipophilicity upon reduction is higher with *ortho* than with *meta* species (Table I). With both isomers, the gain in lipophilicity depends in a bell-shape fashion upon the size of the alkyl chain length; it culminates with butyl porphyrins, and decreases towards ethyl and hexyl analogs [44]. MnTE-2-PyP $^{5+}$ and MnTnHex-2-PyP $^{5+}$ would become ~100-fold more lipophilic upon reduction, while essentially not much gain has been observed with

Table I. Physicochemical properties of MnPs: the metal-centered reduction potential for Mn^{III}P/Mn^{II}P redox couple ($E_{1/2}$), the SOD activity ($O_2^{\cdot-}$ dismuting catalytic rate constant, $\log k_{cat}$), and the lipophilicity of Mn^{III}P and Mn^{II}P described in terms of chromatographic retention factor, R_f , n-octanol-water partition coefficient, $\log P_{ow}$, and the gain in lipophilicity upon Mn^{III}P reduction, $\Delta \log P_{ow}$

Compound	Mn ^{III} P/Mn ^{II} P redox couple $E_{1/2}/mV$ <i>vs</i> NHE ^a	SOD activity $\log k_{cat}$ ($O_2^{\cdot-}$) ^b	Lipophilicity			
			R_f^c	$\log P_{ow}$ (Mn ^{III} P)	$\log P_{ow}$ (Mn ^{II} P)	$\Delta \log P_{ow}$ (upon reduction)
MnTM-4-PyP $^{5+}$ [1,2]	+ 60	6.58	0.064			
MnTE-2-PyP $^{5+}$ [45,46]	+ 228	7.76	0.085	−6.70 ^d	−4.69 ^d	2.01
MnTnHex-2-PyP $^{5+}$ [47,48]	+ 314	7.48	0.394	−2.76 ^e	−0.73 ^d	2.03
MnTnHex-3-PyP $^{5+}$ [46,47]	+ 64	6.64	0.489	−2.06 ^e	−1.74 ^f	0.32

^a $E_{1/2}$ data measured in 0.05 M phosphate buffer, pH 7.8, 0.1 M NaCl. ^bSOD activity measured by the cyt *c* assay in 0.05 M phosphate buffer, pH 7.8, 25 ± 1°C. ^cdata obtained in plastic-backed silica-gel thin-layer chromatography plates eluted with 1:1:8 = KNO₃(sat):H₂O:CH₃CN. ^dCalculated according to equation: $\log P_{ow} = 12.18 \cdot R_f - 7.43$ [46]. ^eDetermined in water/n-butanol ($\log P_{BW}$) system and converted to water/n-octanol system using equation: $\log P_{ow} = 1.55 (\log P_{BW}) - 0.54$ [49]. ^fCalculated according to equation: $\log P_{ow} = 8.78 \cdot R_f - 7.12$ [46].

MnTnHex-3-PyP⁵⁺ (Table I). In turn, the reduced Mn^{II}TnHex-2-PyP⁴⁺ is more lipophilic and may accumulate more within cell than the reduced Mn^{II}TnHex-3-PyP⁴⁺ (Table I). Such considerations are relevant to *in vivo* conditions due to the abundance of reductants; many of them (ascorbate, glutathione, tetrahydrobiopterin, flavoenzymes) could reduce Mn^{III}P [1–5].

This study was designed to elucidate which MnP may be the preferred candidate for further exploration of the therapeutic potential of MnP/ascorbate system. A *meta* and two *ortho* MnPs were compared. The *ortho* compounds used herein are the most studied cationic Mn porphyrins, MnTE-2-PyP⁵⁺ and MnTnHex-2-PyP⁵⁺. MnTE-2-PyP⁵⁺ is 13,500-fold more hydrophilic and has ~100 mV less positive $E_{1/2}$ than MnTnHex-2-PyP⁵⁺. MnTE-2-PyP⁵⁺ has showed efficacy in numerous models of oxidative stress disorders [1–5]. Yet, a lipophilic MnTnHex-2-PyP⁵⁺ is preferred over MnTE-2-PyP⁵⁺ in central nervous system injuries, as well as brain tumours, where transport across the blood brain barrier is critical for its efficacy [18]. Moreover, this compound is advantageous over hydrophilic MnTE-2-PyP⁵⁺ due to its predominant accumulation in mitochondria [5,50–53].

The comparative *E. coli* study of *ortho vs meta* Mn(III) *N*-alkylpyridylporphyrins clearly showed that lipophilicity may compensate for somewhat inferior MnP redox-ability [47]. The *ortho* MnTE-2-PyP⁵⁺ is 10-fold more potent SOD mimic, but *meta* MnTE-3-PyP⁵⁺, with 10-fold lower superoxide dismuting ability, is 10-fold more lipophilic and accumulates therefore 10-fold more within *E. coli* cell. Consequently both *ortho* and *meta* MnTE-2-(and 3)-PyP⁵⁺ are equally efficacious in protecting SOD-deficient *E. coli*. The study clearly showed that *meta* isomers bear therapeutic potential also [47]. They differ from *ortho* analogs predominantly with respect to lipophilicity and reducibility, but with regards to the shape and size of the molecule also; their comparison would allow us to study the impact of such factors upon the anticancer efficacy of MnPs. Therefore, we have chosen to compare the *meta* MnTnHex-3-PyP⁵⁺ to its *ortho* analog MnTnHex-2-PyP⁵⁺.

We have explored 5 different cancer cell lines: human epithelial colorectal adenocarcinoma Caco-2, human epithelial cervical cancer Hela, mouse mammary cancer 4T1, human colon cancer HCT116 and human inflammatory breast cancer SUM149. Inflammatory breast cancer is an aggressive, highly invasive tumour affecting younger women with racial disparity and with one of the worst clinical outcomes among breast cancers [54,55], and is thus of particular interest for therapeutic screening.

Materials and methods

Chemicals

The H₂T-2-PyP and H₂T-3-PyP were purchased from Frontier Scientific. *n*-Hexyl *p*-toluenesulfonate (>98%) was from TCI America. The ethyl *p*-toluenesulfonate (>98%), and tetrabutylammonium chloride hydrate (98%) were from Aldrich. MnCl₂ · 4H₂O (99.7%) was supplied by J. T. Baker. NH₄PF₆ (99.99% pure) was from GFS chemicals. Diethyl ether anhydrous and acetone were from EMD chemicals, while absolute methanol, chloroform, acetonitrile, EDTA and KNO₃ were purchased from Mallinckrodt. *N,N*-dimethylformamide anhydrous (DMF) of 99.8% purity (kept over 4-Å molecular sieves) and plastic-backed silica gel TLC plates (Z122777-25EA) were from Sigma-Aldrich. All chemicals were used as received without further purification. (+)-Sodium L-ascorbate (>98%) and Hoechst 33342 were from Sigma. Due to the sensitivity of the ascorbate towards oxidation, its aqua solution was prepared daily, immediately before the start of an experiment. When the ascorbic acid is dissolved in water the aqueous solution becomes acidic, whereas pH does not change upon dissolving sodium ascorbate. At physiological pH 7.4, ascorbic acid is dissociated and is present as ascorbate. For both reasons, it is more convenient to use sodium ascorbate instead of ascorbic acid.

Tetramethylrhodamine ethyl ester, perchlorate, TMRE was from Molecular Probes. EF5, 2-nitroimidazole was from Cameron Koch, University of Pennsylvania, Philadelphia, PA. Premixed WST-1 cell proliferation reagent from Clontech Laboratories, Inc., was used as received and stored in aliquots at -20°C. The absorbance was measured in a microplate reader (Fluostar optima, BMG labtech).

Cell lines

Human epithelial colorectal adenocarcinoma Caco-2, human epithelial cervical cancer Hela, mouse mammary cancer 4T1, human colon cancer HCT116 were maintained in Alpha-MEM medium supplemented with 10% fetal bovine serum at 37°C. The presence of fetal bovine serum in the medium has not affected the results (data not shown). Human inflammatory breast cancer cell line (mammary epithelial cells) SUM149 was obtained from Asterand, Inc. (Detroit, MI) and was cultured in 6-well plates (Corning Incorporated, Corning, NY) in Ham's F12 supplemented with insulin, hydrocortisone, and 5% fetal bovine serum, FBS until they reached 70–80% confluence. SUM149 are triple negative basal-like cancer cells with activated EGFR and isolated from primary IBC tumour [56]. Previous studies have shown a correlation between ROS generation and sensitivity to a dual EGFR/HER2 kinase inhibitor approved for IBC therapy [55,56].

Mn porphyrins

Synthesis. The general synthetic procedure for *N*-alkylpyridylporphyrins ($H_2TE-2-PyP^{4+}$, $H_2TnHex-2-PyP^{4+}$ and $H_2TnHex-3-PyP^{4+}$) and their Mn complexes ($MnTE-2-PyP^{5+}$, $MnTnHex-2-PyP^{5+}$ and $MnTnHex-3-PyP^{5+}$) were described earlier [3,48]. Briefly, the solution of $H_2T-2-PyP$ ($H_2T-3-PyP$) in anhydrous DMF was stirred with ethyl *p*-toluenesulfonate or *n*-hexyl *p*-toluenesulfonate at $\sim 105^\circ C$. After the reaction was completed (monitored by TLC plates using 1:1:8 = $KNO_{3(sat)}:H_2O:CH_3CN$ as a mobile phase) the reaction mixture was worked up and counterion was replaced by chloride [3,48]. Porphyrins were subsequently metallated using 20-fold molar excess of $MnCl_2$ in basified aqueous medium. The uv/vis, thin-layer chromatography (TLC), ESI-MS and elemental analysis were performed to ensure the identity and purity of MnP preparations.

Stability of MnPs towards oxidative degradation. Stability of MnPs (6 μM) was previously determined in the presence of ascorbate (0.42 mM), and at pH 7.8 maintained by tris buffer on UV-2501 PC Shimadzu spectrophotometer with 0.5 nm resolution [43]. With hexyl analogs the oxidative degradation with 0.2 mM H_2O_2 in 0.1 M tris buffer was also followed.

In vitro studies

WST-1-based cytotoxicity assay. The assay is based on the reduction of tetrazolium salt WST-1 to a water-soluble colored formazan by mitochondrial dehydrogenases in a metabolically active cell. 10,000 viable cells were plated in each well of a 96-plate in Alpha-minimum essential medium (MEM) supplemented with 10% fetal bovine serum. After 24 h in 5% CO_2 at $37^\circ C$, the medium was replaced with 100 μL of fresh complete medium with different concentrations of drugs. A positive control contained the same number of cells in a complete medium with no drug added. A negative control without cells was used as a blank. Because the Caco-2 cells grow slowly, the plates were incubated for 96 h for Caco-2 cells and 48 h for other three cell lines. The doubling time for Caco-2 cells is ~ 62 h (ATCC catalog), while the doubling times for other cell lines are ~ 24 h (Hela) [57], ~ 23 h (4T1) [58] and ~ 16 h (HCT116) [59]. At the end of the incubation, the cells were washed twice with 1X PBS. Then 100 μL of Opti-Media with 10 μL of proliferation reagent WST-1 was added to each well and the plates were incubated at $37^\circ C$ for another 2 h. The absorbance was measured in a microplate reader (Fluostar optima, BMG labtech) at 450/595 nm and the percent viability was calculated from the following equation: $[(A_{\text{sample}} - A_{\text{blank}}) / (A_{\text{control}} - A_{\text{blank}})] \times 100$. The data were analyzed using the SPSS program version 11.5.0. Differences were considered significant with $p < 0.05$.

TMRE cytotoxicity assay. The viability of inflammatory breast cancer cells was assessed using the mitochondrial membrane potential marker tetramethylrhodamine ethyl ester, perchlorate, TMRE. SUM149 cells were cultured in 6-well plates until they reached 70–80% confluence. Cells were treated with either 30 μM $MnTE-2-PyP^{5+}$ or 30 μM $MnTnHex-2-PyP^{5+}$ in the presence and absence of 3 mM ascorbate for 24 h. After incubation, cells were harvested and incubated for 30 min with 500 nM TMRE. Cells were then washed twice with 1% BSA/PBS and analyzed for fluorescence by flow cytometry. At least 25,000 events were collected on a FACScalibur flow cytometer (Beckton Dickinson, Rockville, MD) and analyzed using Cellquest software (Beckton Dickinson). High fluorescence was calculated by setting a gate on the control cells where the peak reached a minimum, and all experimental samples were compared to this control gate.

Clonogenic assay. This assay measured the long-term effect of the MnPs alone or in combination with ascorbate on the overall survival and clonogenicity of the cells. 4T1 mouse breast carcinoma cells and HCT116 human colorectal carcinoma cells were plated in 6-well plates with 3 mL of DMEM complete growth media. Cells were plated at two densities (100 and 300 cells/well) and allowed to attach for 24 h under normal conditions ($37^\circ C$, 5% CO_2). Then the cells were treated with deionized H_2O (vehicle control) or the indicated concentrations of sodium ascorbate (0.5 and 1 mM) and $MnTnHex-2-PyP^{5+}$ (15 and 30 μM) alone or in combination for 24 h. After treatment, the media with drugs were removed and replaced with a fresh 3 mL of DMEM complete growth medium. The cells were then allowed to incubate under normal conditions for 7–10 days, or until the control cells grew colonies of ≥ 50 cells. Then the cells were rinsed with 1X PBS, fixed in 10% methanol-10% acetic acid and stained with a 0.4% crystal violet solution. Colonies with > 50 cells were counted. Plating efficiencies were determined and normalized to the control. Error bars represent standard error. Each experiment was repeated in a triplicate and a one-way ANOVA analysis with a Fisher's PLSD post-hoc test was used to determine significance values ($*p < 0.05$).

$MnTnHex-2-PyP^{5+}$ levels in 4T1 cells. Cells were plated at 1,440,000 cells per plate in 10 mL DMEM (high glucose + 10% FBS) and allowed 24 h to attach (80% confluence). Then the cells were treated with either 0.5 or 1 mM ascorbate or 5, 15 or 30 μM $MnTnHex-2-PyP^{5+}$ or their combination. After 24 h, the media were poured off, cells were rinsed twice with PBS, and 500 μL of Ripa buffer (Sigma #9806, 10x) per plate was added. Cells were then scraped

from plate and transferred to 1.5 mL tubes, incubated on ice for 10 min, and sonicated for 30 s. They were then centrifuged 5 min at 12,000 rpm. 10 μ L of the supernatant was used to determine protein concentration using a Bradford protein assay [60]. The lysate was used for LCMS/MS analysis of MnTnHex-2-PyP⁵⁺ as previously described in details for the analysis of tumour, cytosolic and mitochondrial homogenate [3,44]. The analyses were performed at Duke Comprehensive Cancer Center, Clinical Pharmacology Laboratory on Shimadzu 20A series (LC) and Applied Biosystems MDS Sciex 4000 Q Trap ESI-MS/MS.

Identification of the major species involved in cytotoxicity of MnPs/ascorbate system. In order to identify reactive species involved in cytotoxicity, under above described conditions Caco-2 cells were treated with MnPs/ascorbate system in the presence and absence of 1,500 units/mL of catalase (peroxide scavenger) and 5 mM mannitol (hydroxyl radical scavenger).

In vivo study

Mouse 4T1 breast cancer model. A total of seventy 6–8 week-old female Balb/c mice weighing an average of 22 g (Charles River Laboratories, Raleigh, NC) were used. Tumours were established from a 100 μ L single cell suspension of 10⁷ cells/mL (total of 10⁶ cells) and were injected subcutaneously into the shaved right flank. Tumour volumes were measured daily with vernier digital caliper and calculated with the formula: $V = \text{length} \times \text{width} \times \text{width} \times \pi/6$. Sixty-eight mice were randomly enrolled into the study after the tumour of each mouse had reached a treatment volume of \sim 200 mm³. The mice were divided into four treatment groups: (1) PBS (400 μ L, intraperitoneally), (2) sodium ascorbate (2 g/kg, twice daily, intraperitoneally), (3) MnTnHex-2-PyP⁵⁺ (1 mg/kg, twice daily, subcutaneously), and (4) combination of MnTnHex-2-PyP⁵⁺ (1 mg/kg, twice daily, subcutaneously) and sodium ascorbate (2 g/kg, twice daily, intraperitoneally). In the 4th group, sodium ascorbate was delivered 1 h after the injection of MnTnHex-2-PyP⁵⁺. The doses of MnP and ascorbate chosen were based on previously published *in vivo* experiments [42, 61]. Mice were treated for the whole duration of study (15 days). Once the tumour burden exceeded 2000 mm³, 0.3 mL of EF5 (10 mM, obtained from Cameron Koch, University of Pennsylvania, Philadelphia, PA) was delivered intraperitoneally 2 h prior to sacrificing the animal, followed by intravenous administration of 100 μ L of Hoechst 33342 (20 mg/mL, Sigma, in 0.9% saline) 2 min prior to sacrificing the animal. Tumours were excised and snap frozen using liquid nitrogen. All animal handlings and pro-

cedures were approved from Duke University Institutional Animal Care and Use Committee.

MnTnHex-2-PyP⁵⁺ levels in tumour and muscle. Tumours and muscles (from opposite legs) were homogenized, and proteins removed from tissue with 1% acetic acid in methanol, solvent evaporated and residue reconstituted in a LCMS/MS mobile phase. Analyses were performed on an Applied Biosystems MDS Sciex 3200 Q Trap and 4000 Q Trap LC/MS/MS spectrometer at Duke Comprehensive Cancer Center, Shared Resource PK Labs as described in details elsewhere [3,44].

Immunohistochemistry. The frozen tumours were stored at -80°C and cryosectioned at 10 μ m thickness. These sections were stained using anti-CD31 mAb at a dilution of 1:100 (BD Bioscience) with Alexa Fluor 488 anti-rat IgG (Invitrogen), anti-CD68 Alexa Fluor 647 (Serotec) at a dilution of 1:100, anti-EF5 (obtained from Cameron Koch, University of Pennsylvania, Philadelphia, PA) at a dilution of 1:2 and Hoechst 33342 (Sigma) at a dilution of 1:1000.

Image analysis. Before staining, slides were dried at room temperature and imaged for Hoechst perfusion immediately. Whole tumour fluorescent images for CD31, CD68, EF5 and Hoechst 33342 staining were made using a fluorescence microscope (Axioskop 2plus; Zeiss) equipped with a cooled charge-coupled device digital camera (retiga 1300R; Q-Imaging) at \times 50 magnification. Images acquired from stage scanning were stitched and overlaid for direct comparison of dual fluorescent images using Photoshop. ImageJ software was used to detect the stained cells area. Regions of interest were determined around the viable tumour area.

Results

In vitro studies

Mn porphyrins stability towards oxidative degradation. Among MnPs studied, MnTnHex-3-PyP⁵⁺ is the most unstable one and degrades significantly within 1.5 h in an aqueous system in the presence of 0.42 mM sodium ascorbate as observed by spectral change (Figure 3) [43]. Its *ortho* analog, MnTnHex-2-PyP⁵⁺, is however the most stable towards oxidative degradation. The affinity towards oxidative degradation is due to the fairly low $E_{1/2}$ of MnTnHex-3-PyP⁵⁺ (\sim 250 and 150 mV more negative relative to MnTnHex-2-PyP⁵⁺ and MnTE-2-PyP⁵⁺, respectively) (Table I), which favours the Mn + 3 oxidation state; when reduced, MnTnHex-3-PyP⁴⁺ readily reoxidizes, giving rise to H₂O₂. The same spectral change was observed when MnP

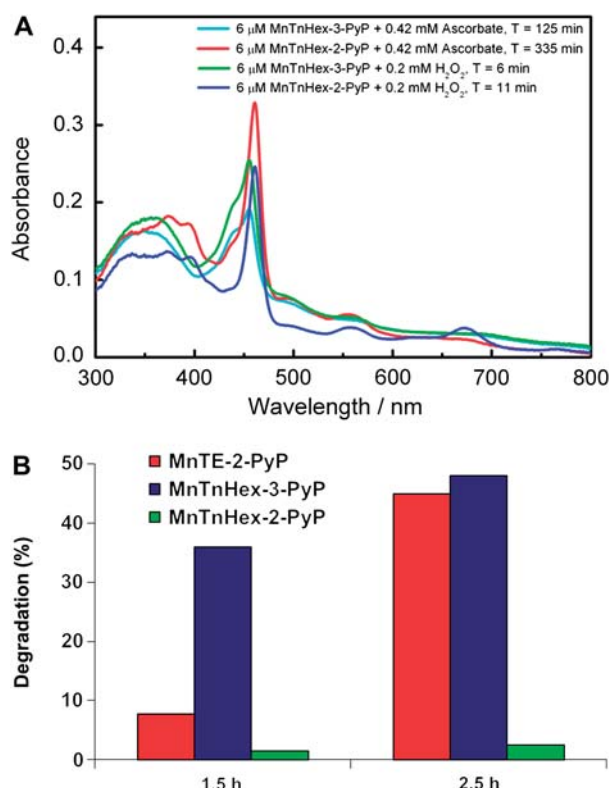


Figure 3. The stability of Mn porphyrins towards oxidative degradation induced by peroxide itself or by the MnP/ascorbate system. MnPs catalyze the ascorbate-induced hydrogen peroxide production. Accumulation of hydrogen peroxide results in the degradation of porphyrin macrocycle. The stability of MnTE-2-PyP⁵⁺, MnTnHex-2-PyP⁵⁺ and MnTnHex-3-PyP⁵⁺ were compared. (A) The uv/vis spectra of MnTnHex-2-PyP⁵⁺ and MnTnHex-3-PyP⁵⁺ were taken at different time points in the presence of either ascorbate or H₂O₂. The conditions were: 6 μM MnPs, 0.42 mM ascorbate, or 0.2 mM H₂O₂, pH 7.8 maintained with 0.1 M tris buffer. The absorption spectra of MnPs with ascorbate mirror those with hydrogen peroxide. (B) The comparison of the stability of all three MnPs towards ascorbate-induced oxidative degradation [43]. The conditions were: 6 μM MnTnHex-2-PyP⁵⁺, 0.42 mM ascorbate in 0.05 M tris buffer [43]. The degradation was assessed at 1.5 and 2.5 h after mixing MnP and ascorbate. The data show that the degradation rates of MnTnHex-2-PyP⁵⁺ and MnTnHex-3-PyP⁵⁺ with ascorbate are the lowest and the highest, respectively, among MnPs explored.

was treated with either ascorbate or H₂O₂ (Figure 3A), undoubtedly indicating that with ascorbate, peroxide was the cause of porphyrin ring degradation (Figure 3) [40,62].

WST-1-based cytotoxicity study of MnP/ascorbate system. Data in Figures 4 and 5 were fitted to a four-parameter logistic equation to determine IC₅₀ values and the results are summarized in Table II. Ascorbate itself was not cytotoxic up to ~3 mM concentration (Figure 5). MnPs alone were not toxic to Caco-2 cells at up to ~40 μM (Figure 4). Therefore, in subsequent studies we have chosen to work with 30 μM concentration of MnPs and 3.3 mM concentration of ascorbate with all cells.

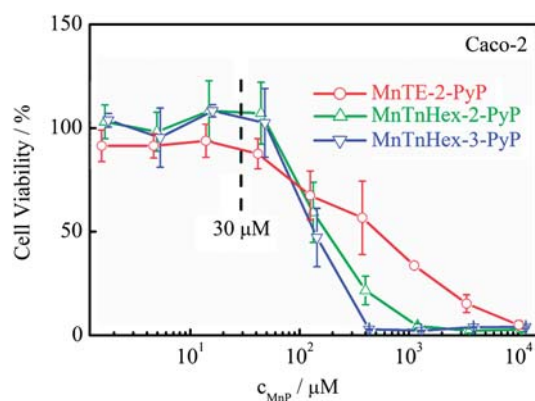


Figure 4. The toxicity of MnPs to Caco-2 cells. Cells were grown for 4 days at a cell density of 10,000 cells/well. Based on these data 30 μM MnPs was chosen for the subsequent studies. Cell viability was measured *via* reduction of tetrazolium salt WST-1 to a water-soluble colored formazan by metabolically active cell.

MnPs. In our earlier *E. coli* studies, in the absence of exogenous reductant, MnTnHex-3-PyP⁵⁺ accumulates several-fold more within the cell but is not accordingly more toxic than is MnTnHex-2-PyP⁵⁺ [47]. Herein, in the absence of ascorbate, despite being ~10-fold more lipophilic than MnTnHex-2-PyP⁵⁺, MnTnHex-3-PyP⁵⁺ is not significantly toxic in its own right, while MnTnHex-2-PyP⁵⁺ is. That suggests that the difference in both their redox properties and bio-availabilities plays a role in their toxicity. Toxicity appears to be cell-type dependent also.

MnPs/ascorbate. Mn porphyrins enhanced cytotoxicity of ascorbate with all tumour cell lines, acting as catalysts of ascorbate-driven peroxide formation (Figures 5, 6 and 7). The combination of MnTnHex-3-PyP⁵⁺ with ascorbate was the least cytotoxic among MnPs studied (Figures 5 and 6), due to its fastest oxidative degradation (Figure 3, Table II).

In all our earlier comparative studies with *E. coli* and with mouse heart and yeast mitochondria [44,50,51], MnTnHex-2-PyP⁵⁺ accumulated more than MnTE-2-PyP⁵⁺ within cell and cellular compartments due to its higher lipophilicity [1–5]. We assumed therefore that it would accumulate more than other MnPs within cancer cells also, and thus exert higher toxicity (Figures 5 and 6). With Mn stabilized in +3 oxidation state relative to MnTnHex-2-PyP⁵⁺ (described by lower $E_{1/2}$, Table I), the MnTE-2-PyP⁵⁺ reoxidizes more rapidly and is thus more efficacious in producing peroxide (Figure 12). Conversely, the MnTnHex-2-PyP⁵⁺ with nearly 100 mV more positive $E_{1/2}$ (Table I) is stabilized in |Mn + 2 oxidation state, and relative to MnTE-2-PyP⁵⁺ disfavours reoxidation which would have otherwise led to the peroxide production. Indeed, based on the slopes of the curves in Figure 5, in the presence of ascorbate, MnTE-2-PyP⁵⁺ appears equally (HCT116, Caco-2) or more cytotoxic (4T1, Hela)

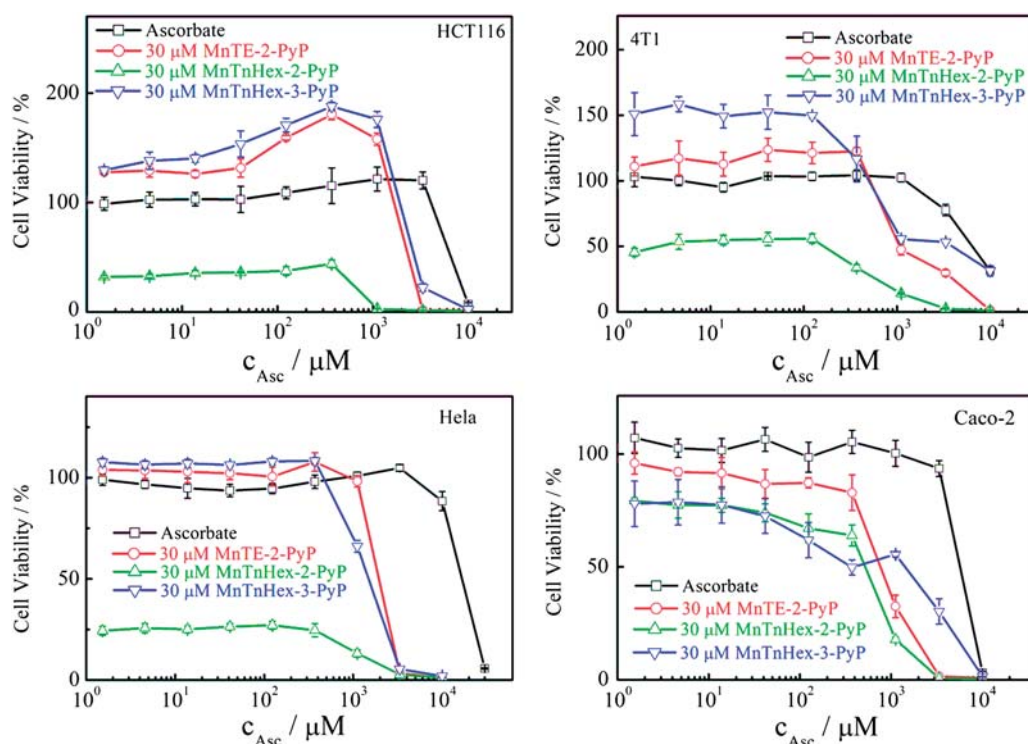


Figure 5. Dose-dependent cytotoxicity of sodium ascorbate in alpha-MEM medium to four tumour cell lines growing for 4 days (Caco-2) or 2 days (HCT116, 4T1 and HeLa) at the density of 10,000 cells/well in 96-well cell culture plates in the absence and presence of 30 μM MnTE-2-PyP⁵⁺, MnTnHex-2-PyP⁵⁺, or MnTnHex-3-PyP⁵⁺ under normoxic conditions. Sodium ascorbate starts to exert cytotoxicity at concentrations > 1 mM. Addition of MnPs markedly potentiated the cytotoxicity of sodium ascorbate. Cell viability was measured *via* reduction of tetrazolium salt WST-1 to a water-soluble colored formazan by metabolically active cell.

than MnTnHex-2-PyP⁵⁺. The same was even more true with inflammatory breast cancer cell line (see Figure 7). Such data strongly suggest that the porphyrin bioavailability/lipophilicity has minor impact on the anticancer effects which are primarily due to its redox ability to cycle with ascorbate in extracellular space/medium. Consequently H₂O₂ is produced, which then enters the cell. The medium has no peroxide-removing systems unless tiny amount of H₂O₂-removing enzymes leaks from the cell [63].

Data in Figures 5 and 6 also show that the low levels of each of MnTnHex-3-PyP⁵⁺, MnTE-2-PyP⁵⁺ (but not MnTnHex-2-PyP⁵⁺) and ascorbate are beneficial to the cell. Such data agree with our earlier observations from *E. coli* studies where some

MnPs increase the growth of wild type presumably *via* easing the cell physiological oxidative burden [43,47]. The pro- *vs* anti-oxidative nature of ascorbate has been discussed in details [64–66]. The production of peroxide *via* metal-catalyzed ascorbate oxidation may be beneficial to cancer cell to some extent allowing it to proliferate, but detrimental if excessive. Such contemplations also point to the complex and not yet fully understood *in vivo* interactions of reactive species and redox-active compounds.

Cytotoxicity of ortho Mn(III) N-alkylpyridylporphyrins/ascorbate in inflammatory breast cancer cell model. Based on the data in 4 other cancer cell lines, the more

Table II. The IC₅₀ values of sodium ascorbate with and without 30 μM MnPs in four cancer cells.

Cancer cell line	IC ₅₀ , mM ^a			
	Asc	Asc + MnTE-2-PyP ⁵⁺	Asc + MnTnHex-2-PyP ⁵⁺	Asc + MnTnHex-3-PyP ⁵⁺
HCT116	4.1 ± 1.0	1.5 ± 0.1	–	2.9 ± 0.1
4T1	6.5 ± 0.3	1.3 ± 0.2	–	2.7 ± 0.3
HeLa	16.4 ± 1.1	1.9 ± 0.1	–	1.3 ± 0.1
Caco-2	5.3 ± 0.5	0.84 ± 0.14 (0.47 ± 0.05)*	0.54 ± 0.08 (0.17 ± 0.02)*	0.87 ± 0.21 (0.14 ± 0.02)*

^aThe IC₅₀ values were calculated relative to the cells growing in medium with neither ascorbate nor MnP added (100% viability). MnTnHex-2-PyP⁵⁺ itself, with no ascorbate added, reduced the cell viability by more than 50% with all cells except Caco-2 (Figure 4).

*The IC₅₀ values for MnPs in the absence of ascorbate.

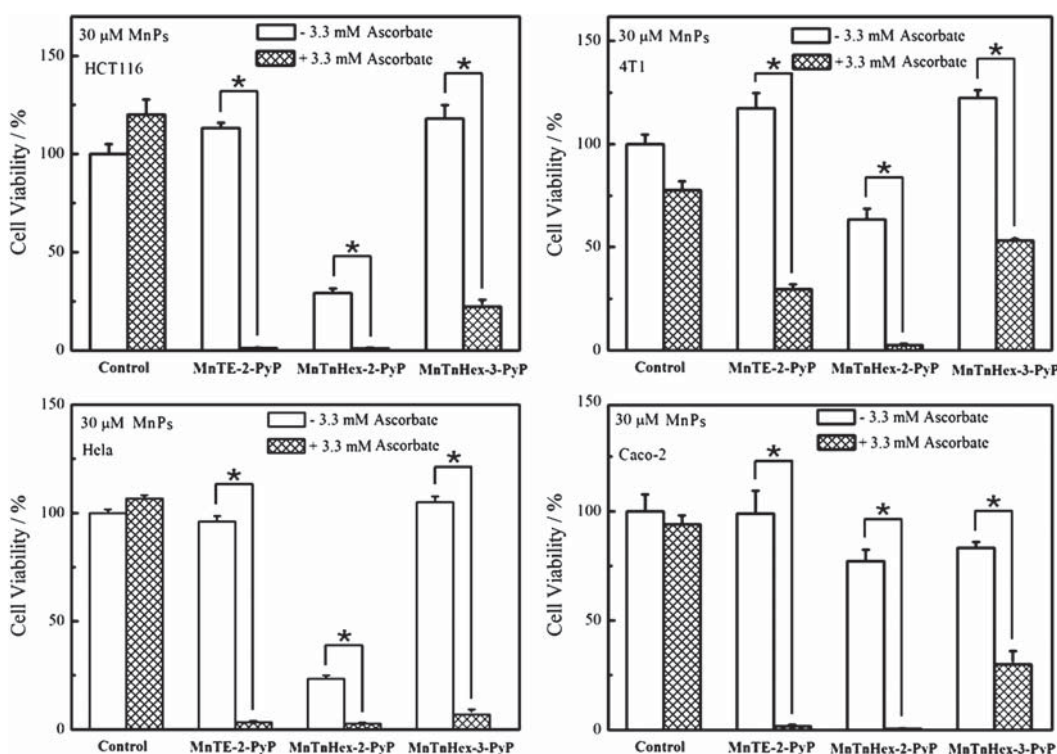


Figure 6. Cytotoxicity of 3.3 mM sodium ascorbate to 4 different cancer cell lines. Cells grew in alpha-MEM medium for 4 days (Caco-2) or 2 days (HCT116, 4T1 and HeLa) at the density of 10,000 cells/well in 96-well cell culture plates in the absence and presence of 30 μM MnTE-2-PyP⁵⁺, MnTnHex-2-PyP⁵⁺, or MnTnHex-3-PyP⁵⁺ under normoxic conditions. Cell viability was measured *via* reduction of tetrazolium salt WST-1 to a water-soluble colored formazan by metabolically active cell and the experiments were performed in triplicate. With Caco-2 cells, MnPs alone did not exert cytotoxicity. With other cell lines 30 μM MnTnHex-2-PyP⁵⁺ itself exerted toxicity. The viability was greatly or fully suppressed when ascorbate was added to the medium. The MnTnHex-3-PyP⁵⁺ was the least cytotoxic when combined with ascorbate. Differences were considered significant with * $p < 0.05$.

efficacious *ortho* isomers were forwarded to the inflammatory breast cancer cell model. MnTE-2-PyP⁵⁺, but not MnTnHex-2-PyP⁵⁺, appeared efficacious (Figure 7) in decreasing cell integrity and viability as measured by mitochondrial membrane potential marker, TMRE. While we do see efficacy of MnTnHex-2-PyP⁵⁺/ascorbate in other cancer cells (see Results, Figure 6), with SUM149 there is none, which suggests that there may be differential response of cancer cell lines to MnPs. Neither of two MnPs was toxic in their own rights. As seen before with Caco-2 cells, ascorbate itself has beneficial effect on the viability of SUM149.

Clonogenicity assessment of the cytotoxicity of MnP/ascorbate system. Ascorbate and MnTnHex-2-PyP⁵⁺ alone did not affect the ability of two different cancer cell lines, 4T1 and HCT 116 cells, to produce colonies (Figure 8). The HCT116 cells seem to be more sensitive than 4T1 cells to the treatment. However, when combined, the treatment significantly decreased cell survival in both cell lines (* $p < 0.0001$). In comparison with WST-1 assay, the clonogenic data show that 30 μM of MnTnHex-2-PyP⁵⁺ is not toxic to 4T1 and HCT116 cells, suggesting that the

cells might have adapted and/or recovered from the stress induced by MnP.

MnTnHex-2-PyP⁵⁺ levels in 4T1 cells. Under given conditions, depending upon the total concentrations of ascorbate and porphyrin and their ratio, up to the 29% more of the MnP was found within the cells when they were treated with MnP/ascorbate compared to MnP treatment alone (Table III). This is somewhat lower than the effect of ascorbate on the MnP accumulation in tumour and muscle (Figure 10B) [44]. This is in agreement with the increased lipophilicity of the reduced Mn^{II}TnHex-2-PyP⁴⁺ relative to oxidized Mn^{III}TnHex-2-PyP⁵⁺ [44]. However, the accumulation of MnP within the cell appears not to be relevant for the efficacy of MnPs in our *in vitro* experiments, because our data indicate that the peroxide produced outside of the cell, in medium, is the main cause of cytotoxicity which agrees with Chen et al conclusions [6] (see Discussion also).

Assuming a cellular volume of 2.19 $\mu\text{L}/\text{mg}$ protein [67], and 0.27 nmole MnP/mg protein determined (Table III), we calculated that when 1.44×10^6 cells in 10 mL plate were treated with 30 μM MnP, the intracellular MnP concentration was 123 μM (0.27×10^{-9} mole/ 2.19×10^{-6} L).

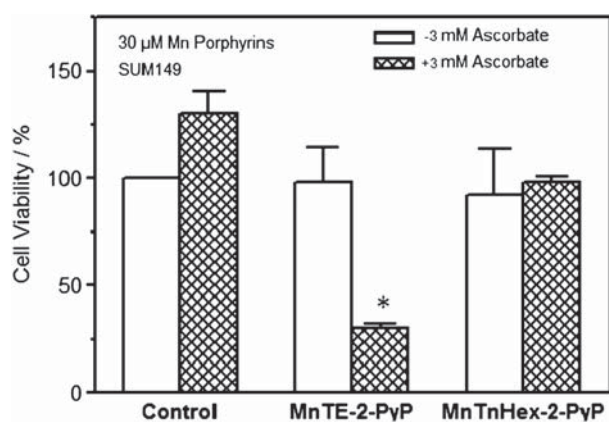


Figure 7. The cytotoxic effects of 30 μM MnTE-2-PyP⁵⁺ and MnTnHex-2-PyP⁵⁺ on the inflammatory breast cancer line SUM149 in the presence of 3 mM ascorbate. Cell viability was assessed *via* measurements of mitochondrial membrane potential marker tetramethylrhodamine ethyl ester perchlorate, TMRE. Cells were incubated with MnPs \pm ascorbate for 24 h. Bars represent mean \pm SEM normalized to DMSO. The student's two-tailed t test was used to calculate p values. Compared to control, the * $p < 0.0001$ for MnTE-2-PyP⁵⁺/ascorbate.

Assuming a volume of a cell of 2000 fL (from the data listed for mouse lymphoblastoid cells, [68]), the total volume occupied by 1.44×10^6 cells was $1.44 \times 10^6 \text{ cells} \times 2000 \times 10^{-15} \text{ L cell}^{-1} = 2.88 \times 10^{-6} \text{ L}$. Then the amount of MnP in $2.88 \times 10^{-6} \text{ L}$ is $3.44 \times 10^{-10} \text{ mole}$ ($123 \times 10^{-6} \text{ mole} \times \text{L}^{-1} \times 2.88 \times 10^{-6} \text{ L}$). Total number of moles of porphyrin in 10 mL medium was 3×10^{-7} ($30 \times 10^{-6} \text{ mole} \times \text{L}^{-1} \times 10^{-2} \text{ L}$). Although the MnP concentration in the cells is ~ 4 times higher than in the medium, the total volume of cells is only tiny fraction of the medium volume. Therefore, the final concentration of MnP in the medium remained essentially the same as initial, $29.97 \mu\text{M}$ ($\{3 \times 10^{-7} - 3.44 \times 10^{-10}\} \text{ mole}/10^{-2} \text{ L}$).

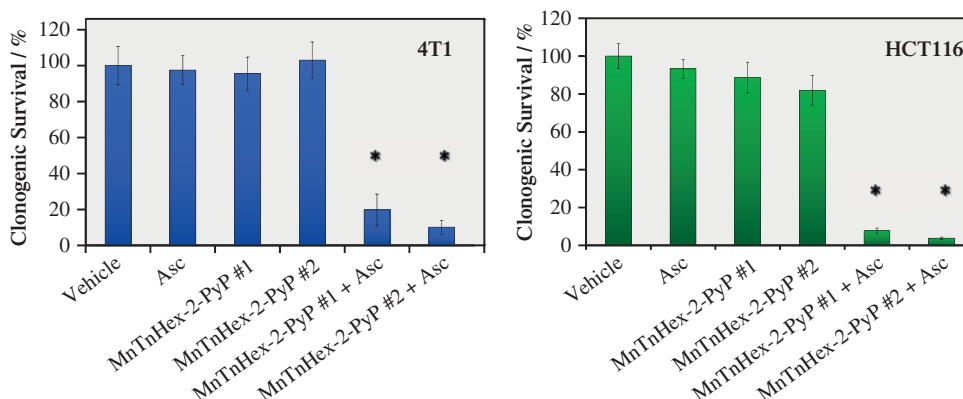


Figure 8. 4T1 mouse mammary cancer cells and HCT116 human colon cancer cells were treated with ascorbate (Asc) or MnTnHex-2-PyP⁵⁺ alone or in combination for 24 h. Clonogenic assays were conducted to assess the effect of MnP/ascorbate on cell survival and proliferation. The combination treatment in both cell lines is significantly more toxic than either of the individual treatments (* $p < 0.001$). HCT116 cells were treated with ascorbate (0.5 mM), MnTnHex-2-PyP⁵⁺ #1 (15 μM) or MnTnHex-2-PyP⁵⁺ #2 (30 μM) alone or in combination for 24 h. 4T1 cells were treated with ascorbate (1 mM), MnTnHex-2-PyP⁵⁺ #1 (15 μM) or MnTnHex-2-PyP⁵⁺ #2 (30 μM) alone or in combination for 24 h.

Identification of the species involved in the cytotoxicity of MnPs/ascorbate system. In order to identify the reactive oxygen species involved in MnPs/ascorbate cytotoxicity, Caco-2 cells were treated with either MnPs or ascorbate alone, or their combination in the presence and absence of catalase (Figure 9A) and mannitol (Figure 9B). Both mannitol and catalase diminished the cytotoxic effects of MnP/ascorbate systems. The effect was somewhat larger with catalase indicating that the peroxide is the major species involved in cytotoxicity. In the presence of metals, H_2O_2 would lead to the production of $\cdot\text{OH}$ radicals (Figure 12). The effect of mannitol on cell viability was only substantial with MnTnHex-3-PyP⁵⁺. The results are in agreement with data reported by Tian et al on *ortho* methyl analog, MnTM-2-PyP⁵⁺. These data also indicate that both lipophilic MnPs, MnTnHex-2-PyP⁵⁺ and MnTnHex-3-PyP⁵⁺, exert fair toxicity to Caco-2 cells in their own rights and presumably *via* production of H_2O_2 and $\cdot\text{OH}$ radical also. In both experiments (Figure 9) MnTnHex-3-PyP⁵⁺ by itself is consistently less toxic than MnTnHex-2-PyP⁵⁺ which is in agreement with data shown in Figures 5 and 6.

In vivo study

Mouse 4T1 breast cancer study of the MnP/ascorbate system. The lipophilic MnTnHex-2-PyP⁵⁺, was shown to accumulate more in cell and in particular in critical cellular compartments – mitochondria than MnTE-2-PyP⁵⁺, and was therefore chosen for the *in vivo* study [5,41,51]. The dose of MnTnHex-2-PyP⁵⁺ used was taken from our previous *in vivo* brain tumour study [69], while the dose chosen for ascorbate (2 g/kg twice daily ip) was taken from the Levine et al study [42]. Levine group has shown clearly that only ascorbate given iv or ip, but

Table III. LCMS/MS analysis of the MnTnHex-2-PyP⁵⁺ levels in the 4T1 tumour cells cultured in the presence or absence of ascorbate.

Exp #	Concentration of MnTnHex-2-PyP (μM) in medium	Concentration of ascorbate (mM) in medium	MnP concentration in tumour cells (nmole/mg protein)	% increase in concentration
1	0	0.5	0.00	
2	0	1	0.00	
3	5	0	0.14	
4	5	0.5	0.15	7.1
5	5	1	0.18	28.6
6	15	0	0.21	
7	15	1	0.27	28.6
8	30	0	0.27	
9	30	1	0.25	none

not per os, achieves therapeutic levels in plasma [42]. The *in vivo* study shows that there is a trend towards tumour growth delay with MnP/ascorbate system, although statistical significance was not reached under our experimental conditions (Figure 10).

The tissue analysis of MnTnHex-2-PyP⁵⁺ shows its higher accumulation in tumour relative to muscle from the opposite leg [44]. Also, ascorbate enhanced MnP accumulation in both tissues by 33% (tumour) and 54% (in muscle), which is due to the increased lipophilicity of the reduced Mn^{II}TnHex-2-PyP⁴⁺ relative to oxidized Mn^{III}TnHex-2-PyP⁵⁺ (Table I) [44]. The effect of ascorbate on MnP accumulation in tumour and muscle is of similar magnitude as the effect of ascorbate on MnP accumulation in 4T1 cells.

Immunohistochemical analysis of tissue sections (stained for microvessel density, perfusion, hypoxia and macrophage). In anti-CD31 staining for microvessels, all

treatment groups showed significant reduction of microvessels compared with PBS group (Figure 11). The microvascular reduction was the highest in MnTnHex-2-PyP⁵⁺/ascorbate group (Figure 11). No differences in EF5 staining, a marker of hypoxia, were detected, suggesting that these treatments did not change the overall hypoxic fraction of these tumours. However, increased perfusion (which suggests favorable drug delivery conditions) as indicated with increased Hoechst staining was observed for the treatment groups compared to the PBS control without reaching statistical significance (Figure 11). The CD68 staining showed that there was increased macrophage infiltration, which implied the increased tumour inflammation when the mice were treated with either ascorbate or MnTnHex-2-PyP⁵⁺/ascorbate (Figure 11). The difference between the control group and MnTnHex-2-PyP⁵⁺/ascorbate group was of marginal significance ($p = 0.0849$).

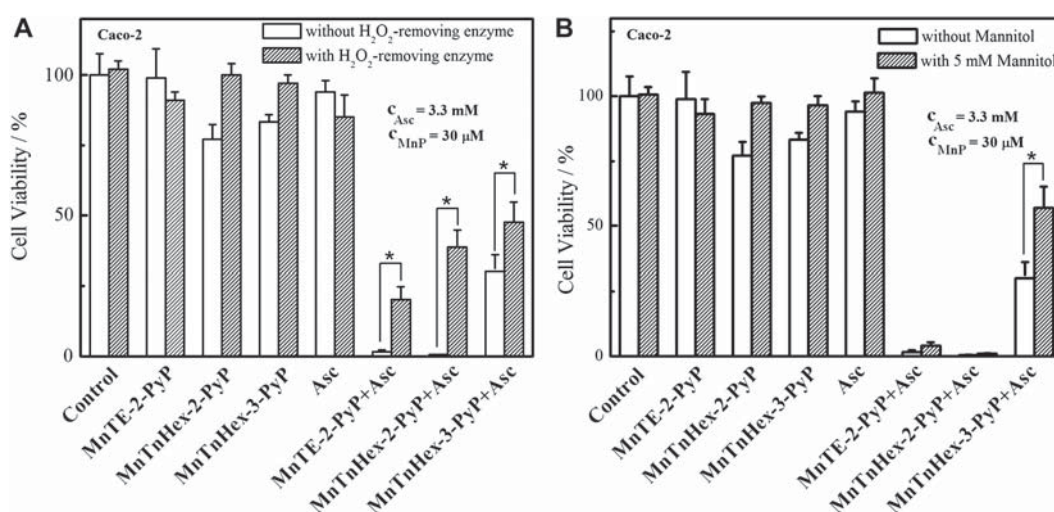


Figure 9. The cytotoxicity of MnP/ascorbate system to Caco-2 cells is due to the production of H₂O₂ and $\cdot\text{OH}$. The 5 mM mannitol ($\cdot\text{OH}$ radical scavenger) blocked significantly the cytotoxicity of MnTnHex-3-PyP⁵⁺ only. The experimental conditions are as stated for Figures 5 and 6. The addition of 1500 U/mL catalase (peroxide scavenger) significantly reduced the cytotoxic effect in all cases, suggesting peroxide as a major damaging species. The Caco-2 cell line was cultured in alpha-MEM supplemented with 10% heat-inactivated FBS, with or without 1500 U/mL catalase or 5 mM mannitol, respectively for 4 days at 37°C. WST-1 assay was used to measure the cell viability. Differences were considered significant with $*p < 0.05$.

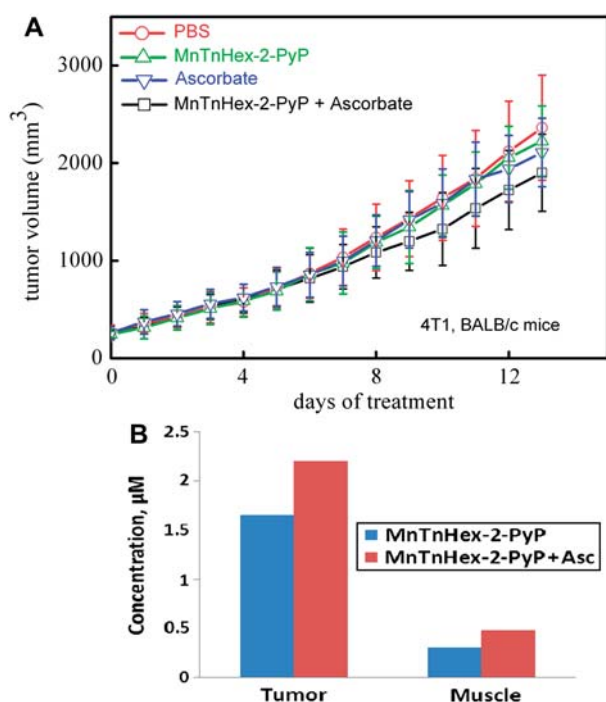


Figure 10. (A) The *in vivo* study of the effect of MnP/ascorbate treatment on the tumour growth delay in 4T1 mammary cancer Balb/c mouse study. Balb/c mice ($n = 17$ for each group) were implanted with 4T1 cells, as described in Materials and Methods. Treatments were started when tumour volume was $\sim 200 \text{ mm}^3$. Four groups received: (1) PBS (400 μL , ip) as control; (2) ascorbate (2 g/kg, twice daily, ip); (3) MnTnHex-2-PyP $^{5+}$ (1 mg/kg, twice daily, sc); and (4) combination of MnTnHex-2-PyP $^{5+}$ (1 mg/kg, twice daily, sc) and ascorbate (2 g/kg, twice daily, ip), respectively. Tumour volumes were measured every day with vernier digital calipers and calculated with the formula $V = \text{length} \times \text{width} \times \text{width} \times \pi/6$ until they reach size of $\sim 2000 \text{ mm}^3$. Under experimental conditions employed, the hypoxia was somewhat potentiated due to the ascorbate-driven oxygen consumption, which presumably counterbalanced the increased tumour oxidative stress and reduction in tumour microvessels and therefore diminished the overall beneficial anticancer effect of MnP/ascorbate. (B) The levels of MnTnHex-2-PyP $^{5+}$ in a mouse tumour and muscle (when mice were treated with either MnP or MnP/ascorbate) expressed in μM in tissue homogenates determined by LCMS/MS method [3,44]. Ascorbate enhanced the MnP accumulation in tumour and muscle by 33% and 54%, respectively.

Discussion

Three Mn porphyrins, MnTE-2-PyP $^{5+}$, MnTnHex-2-PyP $^{5+}$ and MnTnHex-3-PyP $^{5+}$ (Figure 1) with different superoxide dismuting ability ($\log k_{\text{cat}}$), metal-centered reduction potential ($E_{1/2}$), stability towards oxidative degradation and lipophilicity (n-octanol/water partition coefficient, $\log P_{\text{ow}}$) (Table I) were selected for the present study to explore the importance of these parameters in the ascorbate-mediated cancer cell toxicity.

In vitro studies

Ortho vs meta MnPs. *Ortho* isomers, with up to 300 mV more positive $E_{1/2}$ (Table I), are stabilized in

Mn + 2 oxidation state and are thus more readily reducible from Mn $^{\text{III}}$ P to Mn $^{\text{II}}$ P than *meta* isomers. However, once reduced (with ascorbate or $\text{O}_2^{\cdot-}$), the *meta* isomers undergo more rapid reoxidation to Mn $^{\text{III}}$ P than *ortho* porphyrins, with either $\text{O}_2^{\cdot-}$ or O_2 giving rise to H_2O_2 or $\text{O}_2^{\cdot-}$. $\text{O}_2^{\cdot-}$ would subsequently self-dismute or be enzymatically reduced to H_2O_2 . H_2O_2 produced would in turn degrade MnP (Figure 12). Thus, MnTnHex-3-PyP $^{5+}$ appeared the least stable compound among three MnPs explored, and for the same reason the least efficacious catalyst of ascorbate oxidation (Figure 3). Ascorbyl radical, produced in the first step of Mn $^{\text{III}}$ P reduction to Mn $^{\text{II}}$ P, would react with either O_2 or $\text{O}_2^{\cdot-}$; that would again lead to increased peroxide levels (Figure 12). Finally, in a radical-radical reaction, ascorbyl and superoxide would produce H_2O_2 . Due to the large excess of ascorbate over MnP, the major peroxide production would arise from MnP catalysis of ascorbate oxidation.

Ortho MnPs. *Hydrophilic* MnTE-2-PyP $^{5+}$ vs *lipophilic* MnTnHex-2-PyP $^{5+}$. The Mn site of MnTnHex-2-PyP $^{5+}$, with $\sim 100 \text{ mV}$ more positive $E_{1/2}$ relative to MnTE-2-PyP $^{5+}$, is more reducible and thus is more stable in reduced Mn + 2 oxidation state [48] (Table I). Further, longer alkyl chains obviously hinder the approach of H_2O_2 towards metal site and therefore this porphyrin is by far the most stable against oxidative degradation (Figure 3). Such sterical conformation may hinder approach of ascorbate as well. By disfavoring reoxidation, MnTnHex-2-PyP $^{5+}$ produces less peroxide than MnTE-2-PyP $^{5+}$, and is thus less cytotoxic, *i.e.* less efficacious in killing cancer cell. Our earlier *E. coli* data [47,81] showed that MnTnHex-2-PyP $^{5+}$ accumulates to a much higher degree within cell than MnTE-2-PyP $^{5+}$, thereby exerting more toxicity in its own right (Figures 5 and 6) for at least two reasons. Firstly, it has the higher micellar character and could damage cellular membranes [47]. Secondly, the data shown in Figure 9 indicate that, at least in part, MnTnHex-2-PyP $^{5+}$ toxicity is also due to the production of peroxide and hydroxyl radical as it is reversed upon the addition of catalase and mannitol. Taken together the data imply that lipophilicity/bioavailability has only minor impact on the anticancer effects of an *in vitro* MnP/ascorbate system, and that it is the peroxide produced in the medium (extracellular space) that enters the cell and exerts there the cytotoxic effects [42,66,82]. The conclusion is strengthened with the data on inflammatory breast cancer cell line (Figure 7), where none of the two Mn porphyrins alone are toxic, and only MnTE-2-PyP $^{5+}$ /ascorbate was efficacious.

As production of peroxide is related to the $E_{1/2}$ of MnP, one may conclude that the optimal $E_{1/2}$ of an ideal compound, being somewhere around $+200 \text{ mV}$ vs NHE, would allow it to undergo numerous cycles

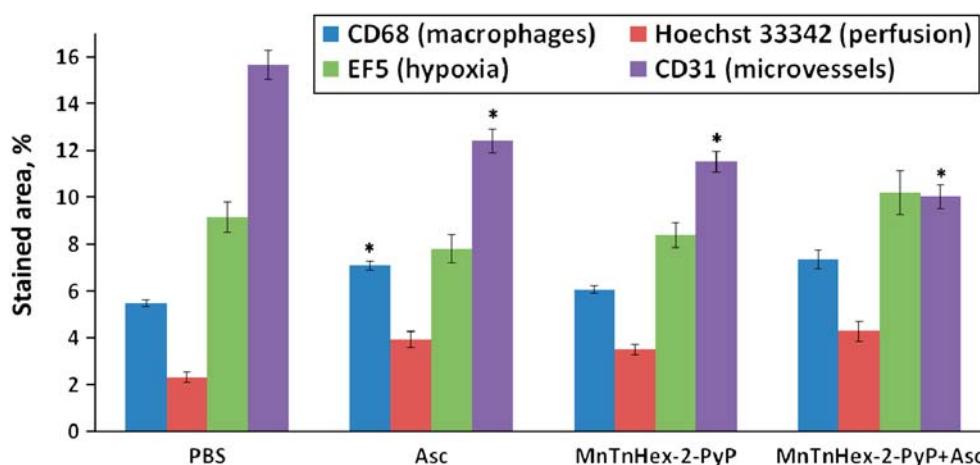


Figure 11. Histograms of stained areas of microvessels (CD31), hypoxia (EF5), perfusion (Hoechst 33342) and macrophage infiltration (CD68). The differences for staining fractions between each treatment groups were determined by the Mann-Whitney test. Differences were considered to be statistically significant if $*p < 0.05$. The difference between the control group and MnTnHex-2-PyP⁵⁺/ascorbate group was of marginal significance ($P = 0.0849$).

between +3 and +2 Mn oxidation states before being oxidatively destroyed. Our data support the notion (already elaborated in Introduction) that the same redox property that makes MnP an ideal SOD mimic, would likely make it an ideal catalyst of ascorbate-driven peroxide production, *i.e.* an ideal anticancer agent.

In vivo study

The *in vivo* system, though, is different than *in vitro* and is hard to predict to what degree the cytotoxic action of MnP/ascorbate may happen in extra- relative to intracellular space. Bioavailability may play a larger role in an *in vivo* setting. Not much is known about the transport of cationic MnPs, and the inhibition of their uptake which would both affect their bioavailability. *The effects in vivo would arise from the interplay of: (1) stability; (2) reducibility; (3) lipophilicity; (4) cellular distribution; (5) toxicity; and other factors that may affect bioavailability such as solvation, size, size and bulkiness of MnPs.*

Immunohistochemistry data from a 4T1 breast cancer mouse study, in particular those on the macrophage infiltration, undoubtedly show that there is a trend towards increased tumour oxidative stress with the MnP/ascorbate system, which along with decreased microvessel density resulted in a marginal tumour growth suppression (Figure 11). However, hypoxia if any was potentiated due to the ascorbate-driven oxygen consumption, and thus the ability of tumour to progress was maintained [83–85]. In light of the anticancer effects observed earlier with MnTE-2-PyP⁵⁺ in a 4T1 mouse study [61], and with MnTnHex-2-PyP⁵⁺ in a brain tumour study [69], as well as with Chen et al on ascorbate [6,42], the optimization of the MnP/ascorbate system may lead to the more pronounced anticancer effects and strengthen its clinical relevance.

The effects observed *in vitro* and *in vivo* may be best summarized in Figure 13. This and other studies by

Espey et al [89], Tian et al [30], Chen et al [42] as well as our *E. coli* studies [12] confirm that peroxide is a major cytotoxic species arising from the catalysis of ascorbate-driven peroxide formation and oxygen consumption (Figure 12). In a healthy cell, the increased peroxide levels may not present a problem due to the abundance of peroxide-removing enzymes (Figure 12). However, the already compromised anti-oxidative status of the cancer cell [85,90,91] (depicted in Figure 13 as the narrower bell-shape curve relative to normal cell), along with additional oxidative burden (depicted in Figure 13 as the shift of the maximum of bell-shape curve relative to normal cell), would force it to undergo death. Alternatively, the cancer cell may try to fight back and upregulate catalases and peroxidases as did *E. coli* in our recent study when challenged by MnP/ascorbate [27]. The response may be cell type related. Under pathological conditions in non-cancer cells, such pro-oxidative action of MnPs alone (with no exogenously added ascorbate) may be operative also and exert beneficial effects by forcing cell to adapt *via* upregulation of endogenous antioxidative defences as shown by us [12] and others [92]. Note, that in such scenario, mechanism of action would be pro-oxidative while effects would be anti-oxidative. Finally, the most recent work by Dorai et al on rat kidney ischemia/reperfusion injury [93] showed clearly that, when rats were treated with renoprotective mixture containing MnTnHex-2-PyP⁵⁺, growth factors, and mitochondrial amino acids, the whole plethora of endogenous antioxidant systems is upregulated. Why the upregulation of antioxidative defences would happen if porphyrin itself is an oxidant: such data greatly support the pro-oxidative type of MnP action which forces cell to undergo adaptive response alike *E. coli* did [12].

The anticancer effects shown here in an *in vitro* cancer cell model pointed to the extracellular action

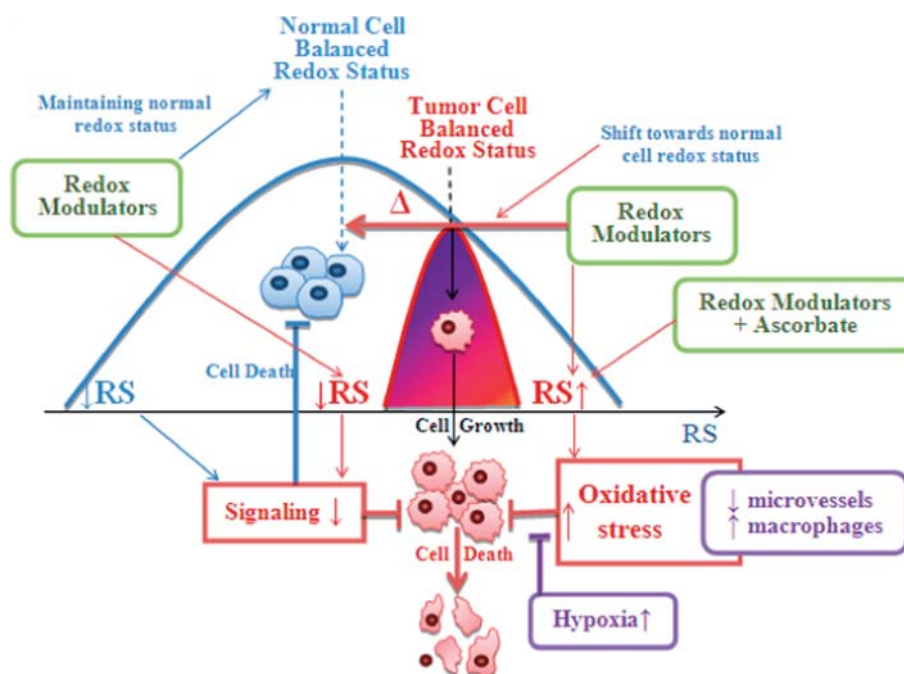


Figure 13. Tumour growth/suppression by MnP as a function of the oxidative stress/levels of reactive species (RS). Depending upon the levels of RS, different cellular events happen: at lower, physiological levels, signalling events predominate, while at very high levels oxidative events prevail. Such scenarios are depicted with two bell shape curves for the normal and cancer cell. Tumour is frequently under oxidative stress; such 'physiological' status is visualized here with the shift of the maximum of its bell shape curve towards higher levels of RS. The increased level of RS is a signal for the upregulation of the genes needed to support tumour angiogenesis and progression [84,85]. Tumour is however vulnerable and any further increase in oxidative burden would force tumour cells to undergo death. The strategy to treat tumours may thus be either to remove RS or to vastly increase their levels. In both cases redox-cycling agents would be efficacious as they can both remove and produce them, acting as anti- or pro-oxidants [5,12]. The latter strategy has already been used in clinic; one example is the combination of ascorbate and redox cycling agent menadione [35,86–88]. HIF-1 α inhibition and VEGF downregulation and tumour angiogenesis suppression is a part of the first strategy where MnP scavenges RS, whereby affecting cell signalling [25,61]. In this work we aimed to show that indeed a redox-able MnP, when combined with ascorbate, exerted anticancer effects *via* increased oxidative burden, acting as a catalyst for ascorbate-driven H₂O₂ production [12]. Further work is needed to comprehend under which conditions MnP would act as antioxidant (removing signalling species) and under which it would kill cells *via* increasing RS levels.

better efficacy relative to MnTnHex-2-PyP⁵⁺; the latter was found more bioavailable in our earlier *in vitro* and *in vivo* studies. Such finding indicates that the bioavailability in this *in vitro* setting has not played a major role in porphyrin efficacy, and suggests that it is the peroxide produced outside of cell that crosses the cell membrane and acts within the cell. Further work is needed to fully comprehend the mechanism/s of action/s of redox-able drugs.

In an *in vivo* 4T1 breast cancer Balb/c mouse study, we observed a trend towards tumour growth suppression by MnP/ascorbate-mediated increased oxidative stress/inflammation, which is at least in part due to the increased macrophages infiltration and reduced microvessel density. The study suggests that further optimization of MnP/ascorbate system for clinical development is warranted.

Acknowledgements

Authors are thankful to Irwin Fridovich for insightful discussions.

Declaration of interest

The authors declare that they have no conflicts of interest and the authors alone are responsible for the content and writing of the article. This study was in great part supported by W.H. Coulter Translational Partners Grant Program. Xiaodong Ye is grateful to the financial support from University of Science and Technology of China during his stay in Professor Kam W. Leong's group at Duke University. Ivan Spasojevic thanks NIH/NCI Duke Comprehensive Cancer Center Core Grant (5-P30-CA14236-29). Diane Fels, Casey Dedeugd and Mark W. Dewhirst are thankful to CA40355-25. Gayathri R. Devi, Katherine M. Aird and Jennifer L. Allensworth acknowledge support of America Cancer Society RSG-08-290-01-CCE, Department of Defense predoctoral Award W81XWH-08-1-0363 and Viral Oncology Training Grant 5T32-CA009111-32 and SPOR in breast cancer grant (5P50-CA068438) at Duke Comprehensive Cancer Center.

References

- [1] Batinic-Haberle I, Reboucas JS, Spasojevic I. Superoxide dismutase mimics: chemistry, pharmacology, and therapeutic potential. *Antioxid Redox Signal* 2010;13:877–918.
- [2] Spasojevic I, Batinic-Haberle I. 2010. Superoxide dismutase mimics. In: Principles of Free Radical Biomedicine. K. Pantopoulos and H. Schipper, eds. Hauppauge, N.Y: Nova Science Publishers, Inc.; Chapter 6, in press.
- [3] Batinic-Haberle I, Reboucas JS, Benov L, Spasojevic I. 2011. Chemistry, biology and medical effects of water soluble metalloporphyrins. In: Kadish, K. M.; Smith, K. M.; Guillard, R., eds. Singapore: World Scientific Handbook of Porphyrin Science;11:291–393.
- [4] Batinic-Haberle I, Spasojevic I, Tse HM, Tovmasyan A, Rajic Z, St. Clair DK, Vujaskovic Z, Dewhurst MW, Piganelli JD. Design of Mn porphyrins for treating oxidative stress injuries and their redox-based regulation of cellular transcriptional activities. *Amino Acids* 2010; doi: 10.1007/s726-010-0603-06.
- [5] Batinic-Haberle I, Rajic Z, Tovmasyan A, Reboucas JS, Ye X, Leong KW, Dewhurst MW, Vujaskovic Z, Benov L, Spasojevic I. Diverse functions of cationic Mn(III) *N*-substituted pyridylporphyrins, recognized as SOD mimics. *Free Radic Biol Med* 2011;51:1035–1053.
- [6] Chen Q, Espey MG, Sun AY, Lee J-H, Krishna MC, Shacter E, Choyke PL, Pooput C, Kirk KL, Buettner GR, Levine M. Ascorbate in pharmacologic concentrations selectively generates ascorbate radical and hydrogen peroxide in extracellular fluid *in vivo*. *Proc Natl Acad Sci USA* 2007;104:8749–8754.
- [7] Forman HJ, Maiorino M, Ursini F. Signaling functions of reactive oxygen species. *Biochemistry* 2010;49:835–842.
- [8] Buettner GR. Superoxide Dismutase in Redox Biology: The Roles of Superoxide and Hydrogen Peroxide. *Anticancer Agents Med Chem* 2011;11:341–346.
- [9] Ferrer-Sueta G, Quijano C, Alvarez B, Radi R. Reactions of manganese porphyrins and manganese-superoxide dismutase with peroxynitrite. *Methods Enzymol* 2002;349:23–37.
- [10] Ferrer-Sueta G, Vitturi D, Batinic-Haberle I, Fridovich I, Goldstein S, Czapski G, Radi R. Reactions of manganese porphyrins with peroxynitrite and carbonate radical anion. *J Biol Chem* 2003;278:27432–27438.
- [11] Ferrer-Sueta G, Batinic-Haberle I, Spasojevic I, Fridovich I, Radi R. Catalytic scavenging of peroxynitrite by isomeric Mn(III) *N*-methylpyridylporphyrins in the presence of reductants. *Chem Res Toxicol* 1999;12:442–449.
- [12] Batinic-Haberle I, Rajic Z, Benov L. A combination of two antioxidants (an SOD mimic and ascorbate) produces pro-oxidative effect forcing *Escherichia coli* to adapt *via* induction of *oxyR* regulon. *Anticancer Agents Med Chem* 2011;11:329–340.
- [13] Semchyshyn H. Hydrogen peroxide-induced response in *E. coli* and *S. cerevisiae*: different stages of the flow of the genetic information. *Cent Eur J Biol* 2009;4:142–153.
- [14] Tse H, Milton MJ, Piganelli JD. Mechanistic analysis of the immunomodulatory effects of a catalytic antioxidant on antigen-presenting cells: Implication for their use in targeting oxidation/reduction reactions in innate immunity. *Free Radic Biol Med* 2004;36:233–247.
- [15] Jaramillo MC, Frye JB, Crapo JD, Briehl MM, Tome ME. Increased manganese superoxide dismutase expression or treatment with manganese porphyrin potentiates dexamethasone-induced apoptosis in lymphoma cells. *Cancer Res* 2009;69:5450–5457.
- [16] Jaramillo MC, Briehl MM, Tome ME. Manganese porphyrin glutathionylates the p65 subunit of NF- κ B to potentiate glucocorticoid-induced apoptosis in lymphoma. *Free Radic Biol Med* 2010;49:S63.
- [17] Sheng H, Yang W, Fukuda S, Tse HM, Paschen W, Johnson K, et al. Long-term neuroprotection from a potent redox-modulating metalloporphyrin in the rat. *Free Radic Biol Med* 2009;47:917–23.
- [18] Sheng H, Spasojevic I, Tse HM, Jung JY, Hong J, Zhang Z, et al. Neuroprotective Efficacy From A Lipophilic Redox-Modulating MnPorphyrin, MnTnHex-2-PyP: Rodent Models of Ischemic Stroke and Subarachnoid Hemorrhage. *J Pharmacol Exp Ther* 2011;338:906–916.
- [19] Jaramillo MC, Briehl MM, Crapo JD, Batinic Haberle I, Tome ME. Manganese porphyrins acts as a pro-oxidant to glutathionylate p65 NF- κ B and potentiate glucocorticoid-induced apoptosis in lymphoma cells. *Free Radic Biol Med*. Submitted.
- [20] Garcia J, Sancheti H, Yap LP, Kaplowitz N, Cadenas E. Regulation of mitochondrial glutathione redox status and protein glutathionylation by respiratory substrates. *J Biol Chem* 2010;285:39646–39654.
- [21] Zweier JL, Chen CA, Druhan LJ. S-glutathionylation reshapes our understanding of endothelial nitric oxide synthase uncoupling and nitric oxide/reactive oxygen species-mediated signaling. *Antioxid Redox Signal* 2011;14:1769–1775.
- [22] Dalle-Donne I, Colombo G, Gagliano N, Colombo R, Giustarini D, Rossi R, Milzani A. S-glutathionylation in life and death decisions of the cell. *Free Radic Res* 2011;45:3–15.
- [23] Tew KD, Manevich Y, Grek C, Xiong Y, Uys J, Townsend DM. The role of glutathione S-transferase P in signaling pathways and S-glutathionylation in cancer. *Free Radic Biol Med* 2011;51:299–313.
- [24] Xiong Y, Uys JD, Tew KD, Townsend DM. S-glutathionylation: From Molecular Mechanisms to Health Outcomes. *Antioxid Redox Signal* 2011;15:233–270.
- [25] Moeller BJ, Cao Y, Li CY, Dewhurst MW. Radiation activates HIF-1 to regulate vascular radiosensitivity in tumors: role of reoxygenation, free radicals, and stress granules. *Cancer Cell* 2004;5:429–441.
- [26] Zhao Y, Chaiswing L, Oberley TD, Batinic-Haberle I, St Clair W, Epstein CJ, St Clair D. A mechanism-based antioxidant approach for the reduction of skin carcinogenesis. *Cancer Res* 2005;65:1401–1405.
- [27] Bottino R, Balamurugan AN, Tse H, Thirunavukkarasu C, Ge X, Profozich J, et al. Response of human islets to isolation stress and the effect of antioxidant treatment. *Diabetes* 2004;53:2559–2568.
- [28] Oliver KM, Garvey JF, Teck Ng C, Veale DJ, Fearon U, Cummins EP, Taylor CT. Hypoxia activates NF- κ B-dependent gene expression through the canonical signaling pathway. *Antioxid Redox Signal* 2009;11:2058–2064.
- [29] Chen Q, Espey MG, Krishna MC, Mitchell JB, Corpe CP, Buettner GR, et al. Pharmacologic ascorbic acid concentrations selectively kill cancer cells: action as a pro-drug to deliver hydrogen peroxide to tissues. *Proc Natl Acad Sci USA* 2005;102:13604–13609.
- [30] Tian J, Peehl DM, Knox SJ. Metalloporphyrin synergizes with ascorbic acid to inhibit cancer cell growth through fenton chemistry. *Cancer Biother Radiopharm* 2010;25:439–448.
- [31] Verrax J, Buc Calderon P. Pharmacologic concentrations of ascorbate are achieved by parenteral administration and exhibit antitumoral effects. *Free Radic Biol Med* 2009;47:32–40.
- [32] Hempel N, Ye H, Abessi B, Mian B, Melendez JA. Altered redox status accompanies progression to metastatic human bladder cancer. *Free Radic Biol Med* 2009;46:42–50.
- [33] Hempel N, Carrico PM, Melendez JA. Manganese Superoxide Dismutase (Sod2) and Redox-Control of Signaling Events that Drive Metastasis. *Anticancer Agents Med Chem* 2011;11:191–201.
- [34] Fridovich I. Superoxide dismutases: anti- versus pro-oxidants? *Anticancer Agents Med Chem* 2011;11:175–177.
- [35] Verrax J, Beck R, Dejeans N, Glorieux C, Sid B, Pedrosa RC, et al. Redox-Active Quinones and ascorbate: An innovative cancer therapy that exploits the vulnerability of cancer cells to oxidative stress. *Anticancer Agents Med Chem* 2011;11:213–221.

- [36] Levine M, Wang Y, Padayatty S, Morrow J. A new recommended dietary allowance of vitamin C for healthy young women. *Proc Natl Acad Sci USA* 2001;98:9842–9846.
- [37] Levine M, Conry-Cantilena C, Wang Y, Welch RW, Washko PW, Dhariwal KR, et al. Vitamin C pharmacokinetics in healthy volunteers: evidence for a recommended dietary allowance. *Proc Natl Acad Sci USA* 1996;93:3704–3709.
- [38] Cullen JJ, Spitz DR, Buettner GR. Comment on “Pharmacologic ascorbate synergizes with gemcitabine in preclinical models of pancreatic cancer,” i.e., all we are saying is, give C a chance. *Free Radic Biol Med* 2011;50:1726–1727.
- [39] Tareen B, Summers JL, Jamison JM, Neal DR, McGuire K, Gerson L, Diokno A. A 12 week, open label, phase I/IIa study using apatone for the treatment of prostate cancer patients who have failed standard therapy. *Int J Med Sci* 2008;5:62–7.
- [40] Spasojevic I, Colvin OM, Warshany KR, Batinić-Haberle I. New approach to the activation of anti-cancer pro-drugs by metalloporphyrin-based cytochrome P450 mimics in all-aqueous biologically relevant system. *J Inorg Biochem* 2006;100:1897–1902.
- [41] Ye X, Fels D, Dedeugd C, Dewhirst MW, Leong K, Batinić-Haberle I. The *in vitro* cytotoxic effects of Mn(III) alkylpyridylporphyrin/ascorbate system on four tumor cell lines. *Free Radic Biol Med* 2009;47:S136.
- [42] Chen Q, Espy MG, Sun AY, Pooput C, Kirk KL, Krishna MC, et al. Pharmacologic doses of ascorbate act as pro-oxidant and decrease growth of aggressive tumor xenografts in mice. *Proc Natl Acad Sci USA* 2008;105:11105–11109.
- [43] Tovmasyan A, Rajic Z, Spasojevic I, Reboucas JS, Chen X, Sheng H, et al. Methoxy-derivatization of alkyl chains increases the efficacy of cationic Mn porphyrins. Synthesis, characterization, SOD-like activity, and SOD-deficient *E. coli* study of *meta* Mn(III) *N*-methoxyalkylpyridylporphyrins. *Dalton Trans* 2011;40:4111–4121.
- [44] Spasojevic I, Kos I, Benov LT, Rajic Z, Fels D, Dedeugd C, et al. Bioavailability of metalloporphyrin-based SOD mimics is greatly influenced by a single charge residing on a Mn site. *Free Radic Res* 2011;45:188–200.
- [45] Batinić-Haberle I, Benov L, Spasojević I, Hambright P, Crumbliss AL, Fridovich I. Relationship among redox potentials, proton dissociation constants of pyrrolic nitrogens, and *in vivo* and *in vitro* superoxide dismutating activities of manganese(III) and iron(III) water-soluble porphyrins. *Inorg Chem* 1999;38:4011–4022.
- [46] Kos I, Rebouças JS, DeFreitas-Silva G, Salvemini D, Vujasković Z, Dewhirst MW, et al. Lipophilicity of potent porphyrin-based antioxidants: comparison of *ortho* and *meta* isomers of Mn(III) *N*-alkylpyridylporphyrins. *Free Radic Biol Med* 2009;47:72–78.
- [47] Kos I, Benov L, Spasojević I, Rebouças JS, Batinić-Haberle I. High lipophilicity of *meta* Mn(III) *N*-alkylpyridylporphyrin-based superoxide dismutase mimics compensates for their lower antioxidant potency and makes them as effective as *ortho* analogues in protecting superoxide dismutase-deficient *Escherichia coli*. *J Med Chem* 2009;52:7868–7872.
- [48] Batinić-Haberle I, Spasojević I, Stevens RD, Hambright P, Fridovich I. Manganese(III) *meso*-tetrakis(*ortho*-*N*-alkylpyridyl) porphyrins. Synthesis, characterization, and catalysis of O₂^{•-} dismutation. *J Chem Soc Dalton Trans* 2002;2689–2696.
- [49] Engelmann FM, Rocha SVO, Toma HE, Araki K, Baptista MS. Determination of *n*-octanol/water partition and membrane binding of cationic porphyrins. *Int J Pharm* 2007;329:12–18.
- [50] Spasojevic I, Yumin C, Noel T, Yu I, Pole MP, Zhang L, et al. Mn porphyrin-based SOD mimic, MnTE-2-PyP⁵⁺ targets mouse heart mitochondria. *Free Radic Biol Med* 2007;42:1193–1200.
- [51] Spasojevic I, Li AM, Tovmasyan A, Rajic Z, Salvemini D, St. Clair D, et al. Accumulation of porphyrin-based SOD mimics in mitochondria is proportional to their lipophilicity. *S. cerevisiae* study of *ortho* Mn(III) *N*-alkylpyridylporphyrins. *Free Radic Biol Med* 2010;49:S199.
- [52] Pollard JM, Reboucas JS, Durazo A, Kos I, Fike F, Panni M, et al. Radioprotective effects of manganese-containing superoxide dismutase mimics on ataxia telangiectasia cells. *Free Radic Biol Med* 2009;47:250–260.
- [53] Yu L, Ji X, Derrick M, Drobyshevsky A, Liu T, Batinić-Haberle I, Tan S. Testing new porphyrins in *in vivo* model systems: effect of Mn porphyrins in animal model of cerebral palsy. 6th International Conference on Porphyrins and Phthalocyanines, ICPP-6, New Mexico 2010.
- [54] Woodward WA, Cristofanilli M. Inflammatory breast cancer. *Semin Radiat Oncol* 2009;19:256–265.
- [55] Aird KM, Allensworth JL, Batinić-Haberle I, Lyerly HK, Dewhirst MW, Devi GR. ErbB1/2 tyrosine kinase inhibitor mediates oxidative stress-induced apoptosis in inflammatory breast cancer cells. *Breast Cancer Res Treat*. 2011, DOI 10.1007/s10549-011-1568-1.
- [56] Aird KM, Ghanayem RB, Peplinski S, Lyerly HK, Devi GR. X-linked inhibitor of apoptosis protein inhibits apoptosis in inflammatory breast cancer cells with acquired resistance to an ErbB1/2 tyrosine kinase inhibitor. *Mol Cancer Ther* 2010;9:1432–1442.
- [57] Zocchi E, Daga A, Usai C, Franco L, Guida L, Bruzzone S, et al. Expression of CD38 increases intracellular calcium concentration and reduces doubling time in HeLa and 3T3 cells. *J Biol Chem* 1998;273:8017–8024.
- [58] Yerlikaya A, Erin N. Differential sensitivity of breast cancer and melanoma cells to proteasome inhibitor Velcade. *Int J Mol Med* 2008;22:817–823.
- [59] Zhou Y, Gwadry FG, Reinhold WC, Miller LD, Smith LH, Scherf U, et al. Transcriptional regulation of mitotic genes by camptothecin-induced DNA damage: microarray analysis of dose- and time-dependent effects. *Cancer Res* 2002;62:1688–1695.
- [60] Noble JE, Bailey MJA. Quantitation of Protein. *Methods Enzymol* 2009;463:73–95.
- [61] Rabbani ZN, Spasojevic I, Zhang X, Moeller BJ, Haberle S, Vasquez-Vivar J, et al. Antiangiogenic action of redox-modulating Mn(III) *meso*-tetrakis(*N*-ethylpyridinium-2-yl) porphyrin, MnTE-2-PyP⁵⁺, via suppression of oxidative stress in a mouse model of breast tumor. *Free Radic Biol Med* 2009;47:992–1004.
- [62] Nam W, Jin SW, Lim MH, Ryu JY, Kim C. Anionic ligand effect on the nature of epoxidizing intermediates in iron porphyrin complex-catalyzed epoxidation reactions. *Inorg Chem* 2002;41:3647–3652.
- [63] Sandstrom PA, Buttke TM. Autocrine production of extracellular catalase prevents apoptosis of the human CEM T-cell line in serum-free medium. *Proc Natl Acad Sci U S A*. 1993;90:4708–4712.
- [64] Gutteridge JM, Halliwell B. Antioxidants: Molecules, medicines, and myths. *Biochem Biophys Res Commun* 2010;393:561–564.
- [65] Halliwell B. Vitamin C: poison, prophylactic or panacea? *Trends Biochem Sci* 1999;24:255–259.
- [66] Halliwell B, Gutteridge JMC. 2007. *Free Radicals in Biology and Medicine*. 4th ed. New York: Oxford University Press.
- [67] Stoll B, Gerok W, Lang F, Häussinger D. Liver cell volume and protein synthesis. *Biochem J*. 1992;287:217–222.
- [68] Tzur A, Kafri R, LeBleu VS, Lahav G, Kirschner MW. Cell Growth and Size Homeostasis in Proliferating Animal Cells. *Science*. 2009;325:167–171.
- [69] Keir ST, Dewhirst MW, Kirkpatrick JP, Bigner DD, Batinić-Haberle I. Cellular redox modulator, Mn(III) *meso*-tetrakis(*N*-*n*-hexylpyridinium-2-yl)porphyrin, MnTnHex-2-PyP⁵⁺ in the treatment of brain tumors. *Anticancer Agent Med Chem* 2011;11:202–212.

- [70] Miller DM, Buettner GR, Aust SD. Transition metals as catalysts of "autoxidation" reactions. *Free Radic Biol Med* 1990; 8:95–108.
- [71] Buettner GR. In the absence of catalytic metals ascorbate does not autoxidize at pH 7: ascorbate as a test for catalytic metals. *J Biochem Biophys Meth* 1988;16:27–40.
- [72] Miller DM, Aust SD. Studies of ascorbate dependent, iron catalyzed lipid peroxidation. *Arch Biochem Biophys* 1989;271: 113–119.
- [73] Buettner GR. Ascorbate autoxidation in the presence of iron and copper chelates. *Free Rad Res Commun* 1986; 1:349–353.
- [74] Kobayashi N, Saiki H, Osa T. Catalytic electroreduction of molecular oxygen using [5,10,15,20-tetrakis-(1-methylpyridinium-4-yl)porphinato] manganese. *Chem Lett* 1985;14: 1917–1920.
- [75] Batinic-Haberle I, Spasojevic I, Stevens RD, Hambright P, Neta P, Okado-Matsumoto A, Fridovich I. New class of potent catalysts of O_2^- dismutation. Mn(III) methoxyethylpyridyl- and methoxyethylimidazolylporphyrins. *J Chem Soc Dalton Trans* 2004;1696–1702.
- [76] Bielski BHJ, Allen AO, Schwarz HA. Mechanism of the disproportionation of ascorbate radicals. *J Am Chem Soc* 1981; 103:3516–3518.
- [77] Williams NH, Yandell JK. Outer-sphere electron-transfer reactions of ascorbate anions. *Austr J Chem* 1982;35:1133–1144.
- [78] Cabelli DE, Bielski BHJ. Kinetics and mechanism for the oxidation of ascorbic acid/ascorbate by HO_2/O_2^- (hydroperoxyl/superoxide) radicals. A pulse radiolysis and stopped-flow photolysis study. *J. Phys. Chem* 1983;87:1809–1812.
- [79] Nadezhdin AD, Dunford HB. The oxidation of ascorbic acid and hydroquinone by perhydroxyl radicals. A flash photolysis study. *Can J Chem* 1979;57:3017–3022.
- [80] Nishikimi M. Oxidation of ascorbic acid with superoxide anion generated by the xanthine-xanthine oxidase system. *Biochem Biophys Res Commun* 1975;63:463–468.
- [81] Okado-Matsumoto A, Batinic-Haberle I, Fridovich I. Complementation of SOD deficient *Escherichia coli* by manganese porphyrin mimics of superoxide dismutase. *Free Radic Biol Med* 2004;37:401–410.
- [82] Ranzato E, Biffo S, Burlando B. Selective ascorbate toxicity in malignant mesothelioma: a redox Trojan mechanism. *Am J Respir Cell Mol Biol* 2011;44:108–117.
- [83] Liao D, Johnson RS. Hypoxia: a key regulator of angiogenesis in cancer. *Cancer Metastasis Rev* 2007;26:281–90.
- [84] Lu X, Kang Y. Hypoxia and hypoxia-inducible factors: master regulators of metastasis. *Clin Cancer Res* 2010;16: 5928–5935.
- [85] Reuter S, Gupta SC, Chaturvedi MM, Aggarwal BB. Oxidative stress, inflammation, and cancer: how are they linked? *Free Radic Biol Med* 2010;49:1603–1616.
- [86] Beck R, Pedrosa RC, Dejeans N, Glorieux C, Levêque P, Gallez B, et al. Ascorbate/menadione-induced oxidative stress kills cancer cells that express normal or mutated forms of the oncogenic protein Bcr-Abl. An *in vitro* and *in vivo* mechanistic study. *Invest New Drugs* 2011;29: 891–900.
- [87] Beck R, Verrax J, Gonze T, Zappone M, Pedrosa RC, Taper H, et al. Hsp90 cleavage by an oxidative stress leads to its client proteins degradation and cancer cell death. *Biochem Pharmacol* 2009;77:375–83.
- [88] Verrax J, Taper H, Buc Calderon P. Targeting cancer cells by an oxidant-based therapy. *Curr Mol Pharmacol* 2008; 1:80–92.
- [89] Espey MG, Chen P, Chalmers B, Drisko J, Sun AY, Levine M, Chen Q. Pharmacologic ascorbate synergizes with gemcitabine in preclinical models of pancreatic cancer. *Free Radic Biol Med* 2011;50:1610–1619.
- [90] Brown NS, Bicknell R. Hypoxia and oxidative stress in breast cancer. Oxidative stress: its effects on the growth, metastatic potential and response to therapy of breast cancer. *Breast Cancer Res* 2001;3:323–7.
- [91] Hussain SP, Harris CC. Inflammation and cancer: an ancient link with novel potentials. *Int J Cancer* 2007;121:2373–2380.
- [92] Kim A, Joseph S, Khan A, Epstein CJ, Sobel R, Huang T-T. Enhanced expression of mitochondrial superoxide dismutase leads to prolonged *in vivo* cell cycle progression and up-regulation of mitochondrial thioredoxin. *Free Radic Biol Med* 2010;48:1501–1512.
- [93] Dorai T, Fishman AI, Ding C, Batinic-Haberle I, Goldfarb DS, Grasso M. Amelioration of renal ischemia-reperfusion injury with a novel protective cocktail, *J Urology* 2011, DOI: 10.1016/j.juro.2011.08.010.
- [94] Sun Y, Oberley LW, Elwell JH, Sierra-Rivera E. Antioxidant enzyme activities in normal and transformed mouse liver cells. *Int J Cancer* 1989;44:1028–1033.

This paper was first published online on Early Online on 14 October 2011.